UNIVERSITY OF AMSTERDAM

MSc Biological Science

Limnology and Oceanography

Research Project 2

Distribution and characterization of deep water cyano-bacterial mats occurring along the west coast of Bonaire (Caribbean Netherlands)

Differences between pigments found in deep and shallow mats

by

R.H.W. van Zanten
10547762

January, 2016
42 ECTS
March 2015 - January 2016

Supervisor:
dr. H.W.G. Meesters

Examiner:
dr. P.M. Visser

Assessor:
dr. F.C. van Duyl

IMARES WAGENINGEN UR

NIOZ

IBED

Institute for Biodiversity and Ecosystem Dynamics

Distribution and characterization of deep water cyano-bacterial mats occurring along the west coast of Bonaire (Caribbean Netherlands)

Differences between pigments found in deep and shallow mats

R.H.W. van Zanten BSc [a], dr. H.W.G. Meesters [b] , dr. P.M. Visser [a] & dr F.C. van Duyl [c]
a: Institute for Biodiversity and Ecosystem Dynamics (IBED), PO Box 94248, 1090 GE Amsterdam, The Netherlands,
b: IMARES – Institute for Marine Resources & Ecosystem Studies, PO Box 167, 1790 AD Den Burg Texel, The Netherlands
c: NIOZ – Royal Netherlands Institute for Sea Research, PO Box 59, 1790 AB Den Burg Texel, The Netherlands

Abstract

Areas like the Caribbean reefs are a biodiversity hotspot. Deeper waters are shown to be of importance for the structure and composition of biological marine communities, but until now only a view studies have been performed on mesophotic reefs (30-100m depth). During three exploratory dives in a submarine along the coast of Bonaire, widespread fields of benthic cyanobacterial mats (BCMs) were found from 45m till 90m depth. These mats are dense structures consisting of different microbial organisms, dominated by cyanobacteria. No previous studies are available of such mats at these depths. Therefore the first aim of this study was to map the distribution of deep BCMs along the west coast of Bonaire, including Klein Bonaire, and to gather more bathymetric data. Almost 30% of the Bonairean west coast contained BCMs. Thereof 44% were found in front of Kralendijk or its suburbs along the coast. BCMs were only found on relative flat and sandy bottoms. Therefore it is thought that the presence of flat and sandy bottoms play a key role in the development of BCMs, but pollution associated with populated areas might play an important role as well. More research is needed to investigate how big the effect of pollution on BCMs formation is and if this can be minimized.

Subsequently a BCMs characterisation study was performed. Hereby, the focus was on the light availability in the mesophotic waters and the light-harvesting pigments of BCMs. At 14.5m depth light of 600nm and higher frequencies was almost completely filtered out and at a depth of 61.4m the 5% light intensity left ranged between 460nm and 500nm. While analyzing the phycobilisome pigments, clear PUB and PEB absorption peaks were found, but no clear PC and APC peaks were found, which is unexpected since these pigments are thought to be always present. Therefore it would be interesting to perform more research on the presence of the phycobilisomes in these BCMs, to find an explanation for these results. Twelve hydrophobic pigments were found, including zeaxanthin, which originates from cyanobacteria. Deep samples contained more pigments than shallow samples ($p=0.005$). Moreover, deep samples compared to shallow samples contained on average 47% more of the light absorbing pigment chlorophyll c3 ($p < 2.20^{-16}$) and 62% less of the light protecting pigment zeaxanthin ($p = 4.62^{-8}$). These results are according to expectations and indicate that these BCMs are adapted to the life on the 'dark' mesophotic reefs.

Index

1. Introduction

Reefs on Bonaire

Bonaire is known for its relatively well preserved reefs along the coast. The Atlantic and Gulf Rapid Reef Assessment (AGRRA) classified Bonaire at the start of the 21th century to be one of the four 'better health' reefs out of twenty islands in the Western Atlantic (Kramer, 2003). In 2008 the National Oceanic and Atmospheric Administration (NOAA) referred to the Bonairean reef as 'the most pristine coral reefs in the Caribbean' (NOAA, 2008). But despite these positive words, also on Bonaire reef degradation takes its part. According to Bak et al., (2005) the coral coverage at 10-20m depth on reefs of Curacao and Bonaire decreased significant from approximately 45% in 1973 to less than 20% in 2002. At 30-40m depth coral coverage was slightly more than 20% in 2003 and did not significantly change over the former three decades. This is explained by the thought that shallow waters are more susceptible than deep waters to anthropogenic activities like shoreline development, physical destruction of corals and even ocean warming (Bak et al., 2005).
Areas like the Philippines, the Gulf of Guinea and also the Caribbean are considered to be a biodiversity hotspot, with exceptional diversity of animals and plants (Roberts et al., 2002). Until now shallow reefs ecosystems are better studied than mesophotic reefs (Lesser et al., 2009). Nevertheless, deeper waters are shown to be of importance for the structure and composition of biological marine communities, but not much is known about the flora and fauna of the mesophotic reefs (Feitoza et al., 2005; Slattery et al., 2011; Becking & Meesters, 2014). Therefore the Dutch Ministry of Economic Affairs (EZ) opted to study the mesophotic reef of Bonaire by use of a submarine (Becking & Meesters, 2014). During the three exploratory dives, benthic cyanobacterial mats were found from 45 meters to 90 meters depth. Since benthic cyanobacterial mats are thought to occur in eutrophic waters and can cause phase shifts on the reef, more research on these organisms in these waters is needed (O'Neil et al., 2012).

Cyanobacteria

Cyanobacteria are oxy-photosynthetic bacteria that are thought to exist for at least 3500 million years (Schopf, 2000; Charpy et al., 2012). They occur in almost all environments, ranging from fresh to marine waters as well on terrestrial environments (Stal, 1995; Codd et al., 1999; Whitton & Potts, 2000). They fulfil an important role in primary production, provide the reef with nitrogen through nitrogen fixation and are grazed upon by organisms living on the reef (Glibert & Bronk, 1994; Stal, 1995; Charpy et al., 2012; Paerl & Paul, 2012). Furthermore some particular species play an important role in calcification and decalcification (Riding, 2000). Cyanobacteria occur as planktonic organisms and benthic organisms (Charpy et al., 2012). The group of benthic cyanobacteria include microbialites, endolithic cyanobacteria, symbiotic cyanobacteria, epiphytes and microbial mats. On the west coast of Bonaire cyanobacteria were found in the form of microbial mats, therefore called benthic cyanobacterial mats.
Benthic cyanobacterial mats (BCMs) are dense structures dominated by cyanobacteria, but also consisting of protozoans and other microbial organisms, such as photosynthetic bacteria and sulphur bacteria (Rejmánková & Komárková, 2000; Charpy et al., 2012). Typically they form flat structures of only a few millimetres thick on the sand. Filamentous cyanobacteria form mucilage sheaths and provide habitats for other organisms (Rejmánková & Komárková, 2000; Riding, 2000; Charpy et al., 2012). As a result, a mat is formed wherein different organisms live in symbiosis and provide each other with nutrients (Stal, 1995; Rejmánková & Komárková, 2000 and references therein; Brocke et al., 2015). Because BCMs occur in almost every type of environment, mats differ in their composition (Leão et al., 2012).
During their long existence, cyanobacteria have developed multiple ecophysiologically advanced characteristics that enables them to survive in and adapt to environments subjected to natural and anthropologically induced changes (Hallock, 2005; Paerl & Paul, 2012). They tolerate increasing solar radiation and rising temperatures (Paerl et al., 1985; Hallock, 2005). Moreover, they thrive in nutrient-rich waters. It is known that eutrophication can stimulate proliferation

and result in a cyanobacteria bloom (O'Neil et al., 2012). Nonetheless it is also thought that to trigger a cyanobacterial bloom, rather than only one factor, multiple factors need to be favourable simultaneously (Paerl et al., 1985; Heisler et al., 2008). Tropical reefs cannot handle these former stated rapid environmental changes and are subjected to coral bleaching and coral death (Glynn, 1991; Lesser & Farrell, 2004). Degrading live coral reefs are prone to overgrowth by cyanobacteria and thereby a phase shift from a coral dominated reef to an algae dominated reef occurs (Smith et al., 1998; Gardner et al., 2003; Pandolfi, 2003).

Benthic cyanobacterial mats along the west coast of Bonaire

During three deep exploratory dives with a submersible on the west coast of Bonaire, widespread fields of BCMs were found from 45 meters to 90 meters depth (Becking & Meesters, 2014). No previous studies are available of such mats at these depths. This feeds the suggestion that these BCMs developed at these depths relatively recently. Although the Bonairean reef is in a relative good state, the presence of BCMs on shallow reefs (0-30m) have been related to nutrient excess and organic pollution (Heisler et al., 2008; Paerl et al., 2011; Brocke et al., 2015). An increase in cover of BCMs and benthic algae on shallow reefs, have been reported to concur with a phase shift from coral cover dominance to algal and BCM dominance (Meltvedt & Jadot, 2014). Over the past decennia benthic macroalgae and BCMs tended to increase on the shallow reefs of Curacao and Bonaire, especially in urbanized areas (Nugues & Bak, 2006; Meltvedt & Jadot, 2014; Brocke et al., 2015). To get more insight into the distribution and the reason of appearance of BCMs at mesophotic depths, exploratory research is needed.

The first aim of this study was to map the distribution of deep BCMs along Klein Bonaire and the west coast of Bonaire. In addition, information on bathymetry and bottom characteristics was gathered, to get a better understanding of the distribution of BCMs along the coast. It was investigated whether deep BCMs are a common phenomenon and whether their occurrence could be related to urbanized areas or other potential sources of pollution located along the coast. Furthermore, habitat conditions of deep BCMs (ca 55m depth) were studied and compared to the conditions found on the shallow reef (ca 15m depth). A high abundance of benthic primary producers, such as cyanobacteria, is remarkable at depths of down to 90m, since they need energy from light penetrating the water column for growth and proliferation (Al-Najjar et al., 2012). Light intensity decreases exponentially with water depth and long wavelengths, including the red and yellow spectrum, are absorbed before short wavelengths, including the green and blue spectrum (Al-Najjar et al., 2012). This might cause differences in photo acclimatisation over depth (Tandeau de Marsac, 1977; Everroad et al., 2006). Therefore the second aim of this study was to describe and compare the light availability at the deep and shallow BCM locations. Furthermore, habitat conditions, such as temperature, pH, salinity, conductivity, chlorophyll and the photo-synthetically active radiation (PAR), in the vicinity of deep and shallow BCMs were investigated.

Differences in photopigment composition between BCMs from deep and shallow locations

Phototropic organisms use different pigments to harvest energy from light. Two commonly used pigment are chlorophyll a and b, which harvest energy around 650nm to 700nm (Figure 1)(Raps et al., 1983; Al-Najjar et al., 2012). But these long wavelengths deplete quickly with depth. Cyanobacteria possess light harvesting pigments that absorb energy from 450nm to 660nm, called phycobilisomes (PBS)(Grossman et al., 1993). Ting et al., (2002) describes phycobilisomes as a supramolecular light-harvesting complex that functions as the primary antenna of PSII in red algae and the majority of cyanobacteria. The PBS complex consists of three main biliproteins, namely phycoerythrin (PE), phycocyanin (PC) and allophycocyanin (APC) (Figure 2)(Gantt, 1974; Su & Fraenkel, 1992; MacColl, 1998). Energy is transferred from PE, the outermost biliprotein on the thylakoid membrane, via PC to APC, the base of the PBS molecule, and then transmitted to chlorophyll a of PSII (Gantt, 1981; Grossman et al., 1993; MacColl, 1998). The biliprotein PE can consist of phycourobilin (PUB) and phycoerythrobilin (PEB). These bilins are responsible for absorption peaks around 498nm (PUB) and around 535nm and 567nm (PEB)(Grossman et al., 1993). PC absorbs around 620nm and APC absorbs between

618nm and 673nm, 650nm being most common (Figure 1)(Grossman et al., 1993). Cyanobacteria can adapt to light intensity by changing the amount of pigments, and they can adapt to the available light spectra by changing the PE:PC ratio and the PUB:PEB ratio (Grossman et al., 1993; MacIntyre et al., 2002; Ueno et al., 2015). Therefore the research question was *'What are the differences in the amount and/or the composition of the phycobilisomes between deep and shallow cyanobacterial mats?'.* It was expected that deep mats would contain more PBS (in total) and that the PE:PC ratio and the PUB:PEB ratio would be higher in deep samples than in shallow samples.

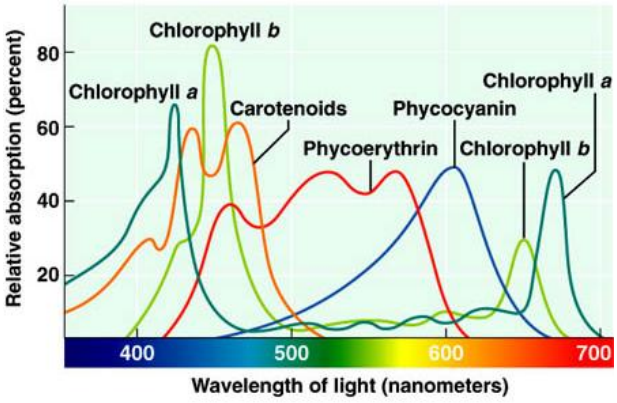

Figure 1. A depict of the relative absorption of different pigments per wavelength

Besides the hydrophilic PBS, cyanobacteria also contain the more common hydrophobic pigments such as chlorophyll a and B-carotene and the cyanobacteria biomarker pigment zeaxanthin, which have different functions (Bianchi et al., 2000; Schlüter et al., 2006). Therefore the research question was *'What are the differences in the amount and/or composition of the hydrophobic pigments between deep and shallow cyanobacterial mats?'*. Because of the low light intensity at the deep sample locations, it is expected that deep samples will contain more light absorption pigments, such as Chlorophyll a and b, and less light protection pigments, such as zeaxanthin and B-carotene.

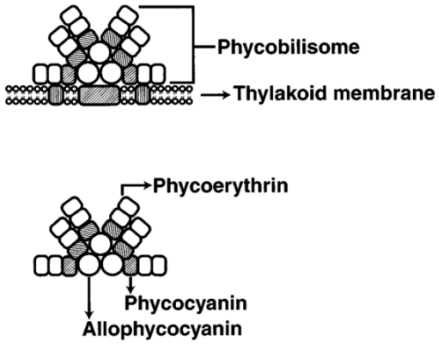

Figure 2. A simple depict of a phycobilisome molecule, attached to PSII on the thylakoid membrane (MacColl, 1998)

2.1 Materials and Methods – BCMs distribution study

Until now only three exploratory deep dives with a submersible were conducted on a part of the west coast of Bonaire. To get more insight into the spread and the reason of appearance of BCMs at mesophotic depths, first a distribution study was performed along the west coast of Bonaire.

Figure 3. 115 waypoints on the west coast of Bonaire. Each dot represents 1 waypoint, located on the coastline

The distribution of deep BCMs was surveyed on 115 waypoints (ca 500m apart) located along the west coast of Bonaire, including Klein Bonaire (Figure 3). The sailing route was created by sailing perpendicular away from a waypoint (WPT) on the coast, until a depth of at least 100 meter was measured, then turning around and in a straight line sailing to the next WPT on the coast (Figure 4). During the transects a Lowrance Depth Finder was used to perform depth measurements and a Seaviewer underwater camera, with a GoPro attached, was deployed at several points to localize the benthic cyanobacterial mats, explained in more detail hereafter. In addition, information on bathymetry and bottom characteristics was gathered, to get a better understanding of the distribution of the deep BCMs along the coast and to gain more knowledge on possible habitat preferences of the cyanobacteria with regard to the structure of the ocean floor and the close activities on land. Based on these results, nine cyanobacterial-inhabited WPTs and three WPTs without cyanobacteria were chosen for a BCMs characterisation study.

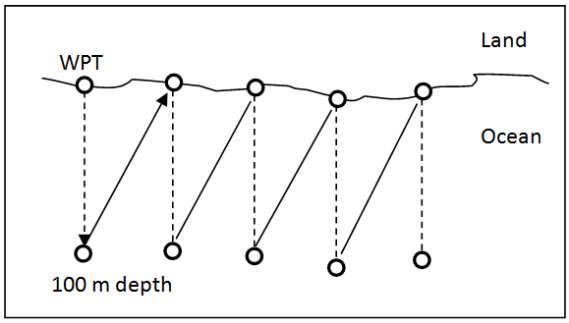

Figure 4. Sailing route between five waypoints at the coast and 100 meter depth (view from above). The distances from the coast differ in length

2.1.1 Lowrance Depth Finder

The Lowrance Depth Finder was used to create a depth chart of the west coast of Bonaire down to at least 100m depth and to keep track of the sailing route. A sonar instrument was attached to the boat and hanging in the water. The sonar instrument was connected to a display and to GPS, hence the water depth and the track of the boat were visible on the display. Information on bathymetry and bottom characteristics was collected until a depth of 100m was reached, whereafter turning around and sailing back to the coast (Figure 4).

2.1.2 Seaviewer

A Seaviewer underwater camera was used to identify the presence of benthic cyanobacterial mats on the west coast of Bonaire through live footage. The camera was deployed multiple times per WPT transect, between 30m and 70m depth and preferably at spots with a flat ocean floor. The information on the depth and the slope of the ocean floor was obtained via the Lowrance Depth Finder. The camera was connected to a monitor on board, to provide live footage and to enable to keep the camera 1m above the ocean floor. An extra under water light was attached to the camera construction, to enhance the quality of the footage. The video data was not stored, but notes on the presence and the biomass of BCMs were taken.

2.1.3 GoPro

A GoPro4 in a customized depth-case was attached to the Seaviewer and set to take pictures with an interval of 10 seconds. If the GoPro was within 1m of the ocean floor, the camera construction was held at this position for at least thirty seconds, to obtain multiple pictures of the area. The addition of an underwater light minimized the noise on the pictures. Pictures were stored and analysed at a later stage.

2.1.4 Data analysis

After the 115 waypoints were examined (Figure 3), the GoPro pictures were analysed. A classification guide was made, allowing to group the WPTs according to the biomass of the benthic cyanobacterial mats recorded during the multiple deployments per WPT (Table 1). From these results WPTs were selected to use during the 'BCMs characterisation study', thereby choosing locations well distributed along the coastline. Furthermore, only WPTs with a classification of '2', '3' or '4' were chosen and the locations had to be accessible for divers. WPTs where BCMs were absent, but with environmental features similar to cyano-WPTs, were chosen as control WPTs used to take water samples and conduct Hydrolab and RAMSES measurements. In addition, information on the bathymetry and bottom characteristics per WPT was collected and used to map the underwater coastline structure of the west coast of Bonaire.

Table 1. Pictures used for the classification of the benthic cyanobacterial mats

Close-up picture	Overview picture	Biomass of mats
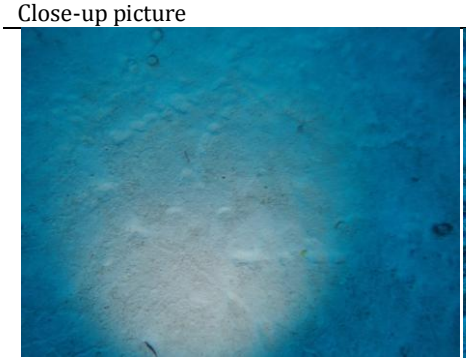	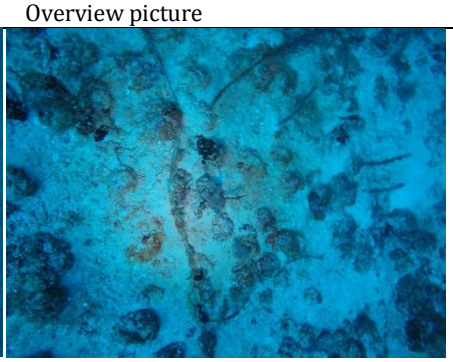	'None' (0)

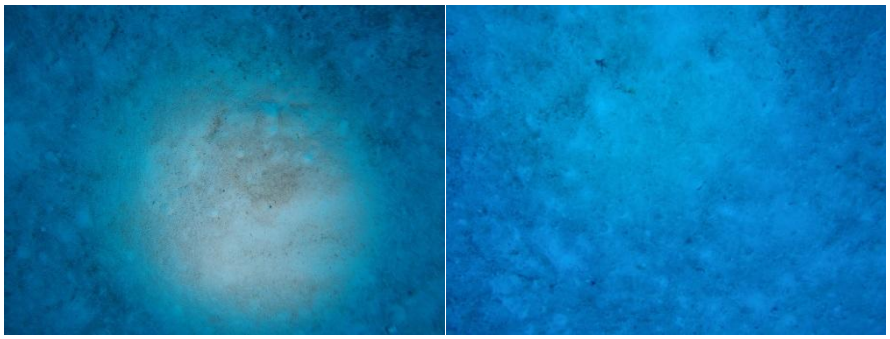

'Very low' (1)

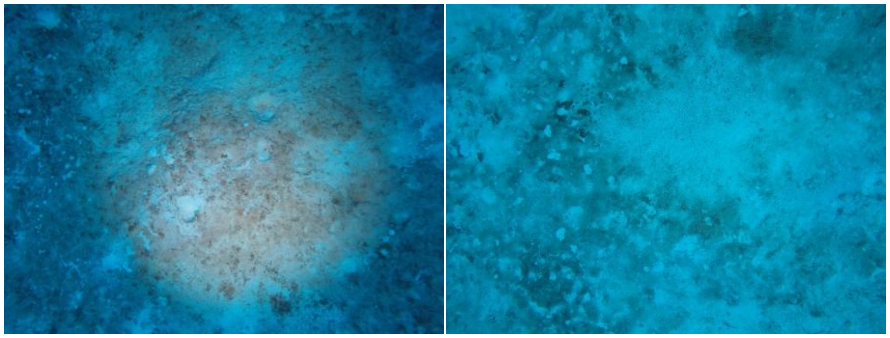

'Low' (2)

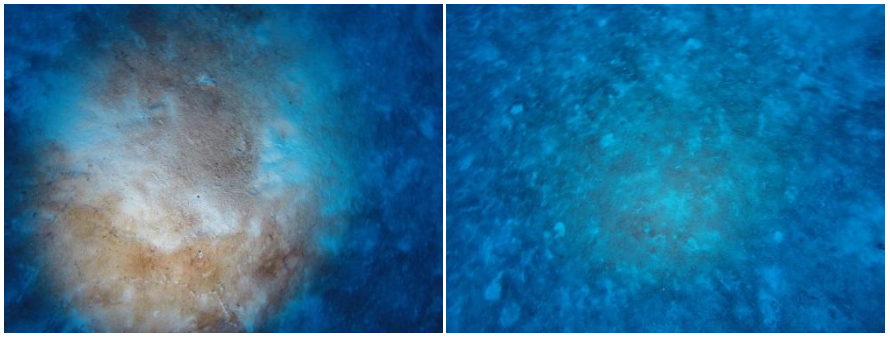

'Intermediate' (3)

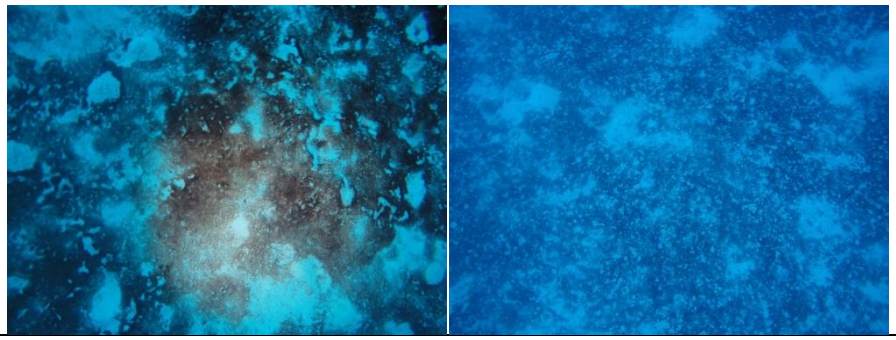

'High' (4)

2.2 Materials and Methods – BCMs characterisation study

At each waypoint, multiple measurements and samples were taken for further research, explained hereafter. Samples and measurements were taken at the following spots (Figure 5):

A: Shallow-reef samples, between 10 and 20 meters depth
B: Deep-reef samples, between 50 and 60 meters depth
C: Control samples, taken between 5 and 10 meters above the ocean floor
D: Extra double-reef samples, taken between 25 and 30 meters depth

'A' and 'B' were taken at the same WPTs (BCMs present), 'C' was taken at control WPTs (BCMs absent) at other locations, and 'D' was taken at the double reef at again another WPT. The '……' indicate that RAMSES and Hydrolab measurements were taken, '○' indicates that water samples were taken and a red circle indicates that water and BCM samples were taken. The

measurements were taken in duplicate, while the measurement device was downcast and when it was upcast. The samples were taken in triplicate. Information on the sampling method of the water samples can be found in the appendix (p35) and information on the exact measuring and sampling time per WPT can be found in Table 3.

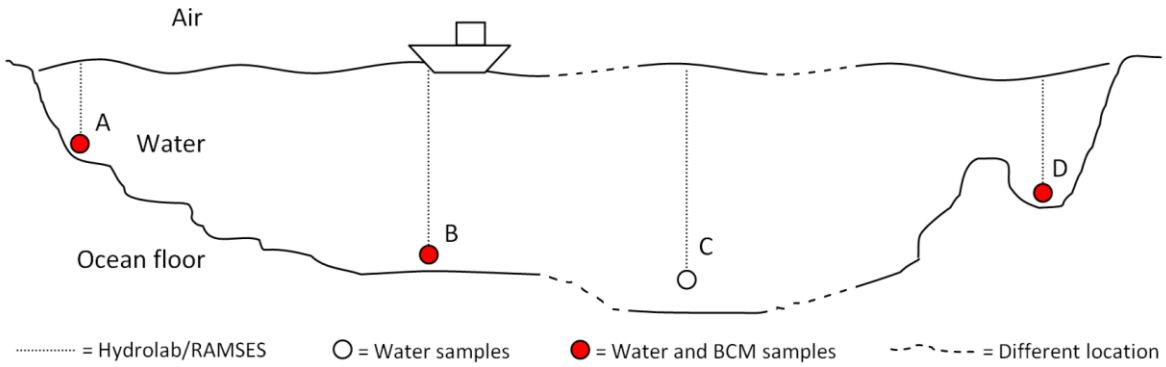

Figure 5. Schematic drawing of the position where the samples and measurements were taken. 'C' is at a different location than 'A' and 'B', as is 'D'

A winch was used to deploy the measurement devices. A length measuring tool was connected to the winch, which gave an indication of the depth of the measurement device while performing the measurements. When a measurement was taken, the exact depth of the device was measured as well. At spots 'A', 'B' and 'D' measurements were taken approximately 2 metres above the bottom, to prevent the measurement device from touching the bottom and thereby suspending organic material originating from the BCM, what would disturb the measurement. At spot 'C' control measurements were taken approximately 7 meters above the ocean floor, which was thought to be below the thermocline.

2.2.1 Hydrolab measurements (Habitat conditions)

The Hydrolab was used to measure pH, temperature (°C), conductivity (mS/cm), salinity (ppt), depth (m), PAR (µE/s/m²) and the amount of chlorophyll (µg/l). The Hydrolab was programmed to automatically take a measurement every 30 seconds, during a time period set up forehand. Measurements were taken according to the depths as presented in Table 2.
Full-day measurements were also taken on land and the PAR measurements were used to create an average light curve on land (Appendix, p37). This average light curve is used to correct differences in the exact time of the data measured under water (Hydrolab measurement timing, Table 3).

2.2.2 RAMSES measurements (Light availability)

The RAMSES (Radiation Measurement Sensor with Enhanced Spectral Resolution) was used to measure the light availability on different depths. It is thought that light intensity changes exponential in the first water layers, therefore measurements were taken with smaller distances in shallow waters and bigger distances with depth (Table 2). The RAMSES was put in a frame with the sensor upwards and lowered on the winch. Measurements were taken and saved on a laptop on board. The first and the last measurement were taken above the water, enabling to recalculate the light availability relative to the surface light at the time of the measurement.

Table 2. Distances between RAMSES/Hydrolab measurements taken at different depths

Depth	Distance between measurements
0 – 2 m	0.5 m
2 – 10 m	1 m
10 – 20 m	2 m
20 – 80 m	5 m

Table 3. An overview of the exact times of the measurements and samples taken per WPT. An explanation of the chosen sites is in the result section of the BCMs distribution study (p15) and the locations are mapped in Figure 9

WPT nr	Where	Biomass	Hydrolab			RAMSES			Samples		
			Date	Deep	Shallow	Date	Deep	Shallow	Date deep	Time deep	Time shallow
126	Klein Bonaire	2	15-5-2015	9:43-10:09	8:51-9:07	15-5-2015	9:25-9:36	9:15-9:21	16-5-2015	9:09-9:24	14:36-15:00
56	Klein Bonaire	Control	1-5-2015	13:36-14:02		1-5-2015	14:07-14:21				
49	North of Kralendijk	2	12-5-2015	8:38-9:05	9:49-10:05	12-5-2015	9:25-9:34	9:40-9:43	11-5-2015	9:04-9:19	15:55-16:25
44	North of Kralendijk	Control	5-5-2015	10:50-11:17		5-5-2015	11:23-11:37				
39	North of Kralendijk	Control	5-5-2015	13:44-14:13		5-5-2015	14:22-14:42				
35	Kralendijk (Harbour)	2	12-5-2015	12:42-13:08	11:59-12:16	12-5-2015	12:26-12:37	12:18-12:22	14-5-2015 (deep) 13-5-2015 (shallow)	9:43-9:58	15:21-15:55
32	Kralendijk (Harbour)	3	8-5-2015	13:20-13:46	12:29-12:45	8-5-2015	12:57-13:15	12:48-12:54	10-5-2015	9:24-9:39	15:07-15:40
30	Kralendijk	4	1-5-2015	11:21-11:47	10:27-10:43	1-5-2015	10:59-11:17	10:47-10:55	3-5-2015	9:28-9:43	15:41-16:05
28	Kralendijk	4	1-5-2015	9:49-10:15	8:38-8:55	1-5-2015	9:26-9:45	9:11-9:20	2-5-2015	9:35-9:50	15:35-16:05
26	Airport of Kralendijk	4	28-4-2015	14:10-14:36	13:51-14:07	28-4-2015	10:36-10:59	10:12-10:31	29-4-2015	9:18-9:32	15:35-16:10
24	Suburb south of Kralendijk	4	5-5-2015	9:36-10:03	8:43-8:59	5-5-2015	9:17-9:32	9:07-9:13	4-5-2015	9:20-9:35	15:23-15:50
15	Salt lakes	3	8-5-2015	9:18-9:45	8:18-8:35	8-5-2015	8:51-9:12	8:41-8:49	9-5-2015	9:32-9:49	15:30-16:00
		Time span	28-4 / 15-5	8:38 / 14:36	8:18 / 14:07	28-4 / 15-5	8:51 / 14:42	8:41 / 12:54	29-4 / 16-5	9:04 / 9:58	14:36 / 16:25

2.2.3 Cyanobacterial mat samples

It was found that the best way to collect the cyanobacterial mat samples was to put them with a fork in a tea sieve, shake a few times to lose a part of the sand through the sieve, and then put the cyanomaterial in a plastic Ziploc bag. This action was repeated until a sufficient amount of BCM was collected. This simple method was particularly useful during the deep dives, since here the sampling time was limited to 3 minutes per replicate. All samples were taken in triplicate and at least 1 meter apart. Judged by their colour, mats with the highest biomass were chosen. The Ziploc bags were put in a dark garbage bag, to prevent the cyanobacterial samples from light damage. After the dive, the Ziploc bags were put in a cool box and multiple vials were filled for different analyses, whereof only the pigment and phycobilisomes analyses are relevant for this research. Gloves were worn and a pair of tweezers was used to collect the cyanomaterial from the samples, thereby minimizing the transfer of sand and seawater. Per sample a 2ml plastic vial was filled with cyanomaterial, to perform analysis on pigments and phycobilisomes. The amount collected per sample differed, therefore some vial were filled with less than 2ml cyano-material. The samples were stored in the dark at -20°C and transported to the Netherlands in a Bio-Freeze bottle.

2.3 Materials and Methods – Sample processing

After the samples were brought to the Netherlands, the samples were processed in the lab and analyses were performed. A part of each pigment sample was taken and set apart for AMINCO analysis. This was done by first slightly thawing the sample, then removing seawater-ice that was on top of the cyanomaterial, mixing the cyanomaterial in the vial and putting 1/3 of the sample in a new vial. This new vial was put in the freezer again. The old vial, containing the remaining 2/3 part, was covered with a lid with two 1mm holes and put in the freezer for an hour. Afterwards the samples were put overnight in the freeze drier till they were dried and stored in the freezer. Hereafter the HPLC analysis and AMINCO analysis were performed and the ash free dry weight (AFDW) was calculated.

2.3.1 HPLC (Hydrophobic pigments)

It was estimated that 50mg of the freeze dried shallow samples and 100mg of the freeze dried deep samples contained enough cyanomaterial to perform the HPLC analysis on. These volumes were weighted and put in a 2ml Eppendorf tube. 400µl 90% acetone and a small amount of 0.5mm beads were added to the tubes. After this, the samples were put for 1 minute in the Beadbeater and ultra-sonicated for 10 minutes at 35KHz in ice water. These last two steps were repeated once. 200µl of 1.5% Tetra-butyl-ammonium acetate and 7.5% Ammonium acetate in MiliQ were added and homogenized on a vortex for 10 seconds. After this, the tubes were centrifuged for 5 minutes at 15000rpm. The samples were kept on ice between the different steps. 70µl of the supernatant was put into a HPLC vial with glass insert and measured over night in a Shimadzu HPCL automatic sampler. Of each sample 20µl was taken, at a flow rate of 0.750ml/min. After the analysis was run, the output consisted of retention time peaks shown at five different wavelengths in the program LabSolutions (Shimadzu). This program was used to compare the sample data to fifteen standard pigments, of which the retention time, absorption spectra and concentration were known. Pigments present in the samples were identified and their concentrations were calculated.

2.3.2 AMINCO (Phycobilisomes – Hydrophilic pigments)

The frozen samples were grinded for 1 minute in a small mortar while 0.5ml 20mM acetate buffer was added. To create this buffer, 0.5M NaAc and 0.5M HAc were mixed till a pH of 5.5 was reached and thereafter diluted with MiliQ water till 20mM. The grinded sample was poured into the 2ml tube while using two times 1ml buffer to rinse the mortar. After leaving the samples extracting in the fridge (4 °C) for 24 hours, the samples were centrifuged for 5 minutes at 150000rpm and 1ml of the supernatant was put in a cuvette. Samples were analysed in a dual

wavelength spectrophotometer (Olis-modernized Aminco DW-2000). A baseline was created by running two cuvettes, containing buffer. Samples were then run against a buffer, with a correction of the baseline. Measurements were taken between 400nm and 750nm with two reads per datum. During this analysis samples were kept on ice between the different steps. After this, the supernatant was pipetted back into the 2ml tube and stored in the freezer at -20°C for later usage.

2.3.3 AFDW

Samples stored after the AMINCO analysis were used to calculate the 'ash free dry weight' per sample, the amount of organic material per gram dry weight. After the samples were frozen again, they were freeze dried overnight and weighted. After 4 hours in an oven at 450°C, the organic material was burned and samples were weighted again. AFDW was calculated according to the following formula:

AFDW = (Sample weight before oven – sample weight after oven) / sample weight before oven

This is used to calculate the amount of pigments and phycobilisomes per gram algae.

2.4 Materials and Methods – Data analysis

The measurements used for the analysis are approaching the water and BCMs sample depths (Figure 5, Figure 18) and labelled according to their depth ('S' = shallow, 'D' = deep, 'C' = control) and to the distance to the sea bottom/BCMs ('0' = closest to BCMs, '5' = 5 meters above BCMs, '10' = about 10 meters above the sea bottom). An overview of the data and the analyses performed can be found in Table 4.

2.4.1 Hydrolab measurements (Habitat conditions)

The two measurements closest to the sample depth were averaged and used for the analysis. Boxplots were created in RStudio, giving an indication of the skewness of the data and possible differences. An average light curve was created by fitting a polynomial trend line in excel on the average data from seven land measurements. A conversion factor relative to the maximum light intensity on land, which was at 12:26:00, was calculated for every measurement between 8:30 and 16:30 (Appendix, p37). PAR measurements at sample depth were recalculated relative to the maximum light intensity.
The extinction coefficient (k) on the ocean floor (D0/S0) was calculated according to

$$I_z = I_0 \cdot e^{-kZ}$$

while using all PAR data of the deployment. The average was taken of the extinction coefficient of the measurements during the downcast and the extinction coefficient of the measurements during the upcast of the Hydrolab. For I_0 the two measurements below 3.5m depth were averaged, because there was too much fluctuation in the PAR measurements between 0m and 3.5m depth.

2.4.2 RAMSES measurements (Light availability)

To create a representative view of the light availability, measurements were grouped and averaged for certain depths (Table 6). These averages were recalculated as relative to the surface light, to show the light intensity left at the calculated depths. The average depth per depth group can be found in Table 7. From this data the wavelength containing the maximum intensity at the deepest measurement of the deep and the shallow deployment was extracted and boarders of 1%, 5%, 33% and 45% remaining light intensity were read off.

2.4.3 AMINCO (Phycobilisomes – Hydrophilic pigments)

The absorption data obtained from the analysis were normalized to their lowest amount of absorption between 600nm and 750nm and recalculated to 100 g^{-1} AFDW.

2.4.4 HPLC (Hydrophobic pigments)

Per sample the amount of pigments per gram organic material was calculated. Boxplots were created in RStudio, giving an indication of the skewness of the data and possible differences. A two-way ANOVA with repeated measures and 'depth' and 'WPT' as factors, including an interaction-factor, was performed on the total amount of pigments and on the amount of separate pigments. If necessary a log10 or sqrt transformation were performed and if zeros were present they were replaced by '½ · lowest measurement'.

Table 4. An overview of the gathered data and the analyses performed

Device	Data	Analysis	Which samples
Hydrolab	Temp/pH/Conductivity/ Salinity/Chlorophyll/PAR at approximate sample depth	- Habitat conditions overview - Relative PAR - Extinction coefficient (k)	- S0/S5/D0/D5/C10 - S0/S5/D0/D5/C10 - S0/D0/C10
RAMSES	Light availability	- (Relative) Light availability of all wavelength at different depth - Max wavelength at lowest point - Boarders of 1%/5% light intensity - Boarders of 33%/45% light intensity	- all measurements - S0/D0/C10 - D0/C10 - S0
AMINCO	Phycobilisomes	- Absorption per sample - Presence of PC/PEII/PEI/PUB/PEB - Wavelength at peak max	- S0/D0 (cyano) - S0/D0 (cyano) - S0/D0 (cyano)
HPLC	Pigments	- Presence of different pigments - Concentration of pigments	- S0/D0 (cyano) - S0/D0 (cyano)
	AFDW	- Used to calculate concentrations of different substances in the samples	- S0/D0 (cyano)

3.1 Results – BCMs distribution study

3.1.1 Depth chart

The data collected with the Lowrance Depth Finder was analysed by ir. H.J. Stuiver (Laboratory of Geo-information Science and Remote Sensing, Wageningen University) with ArcMap, while implementing other bathymetric data and elevation data from land. The depth chart is still under construction but an impression can be found in Figure 6, which shows a part of Klein Bonaire on the left and the area of Kralendijk on the right.

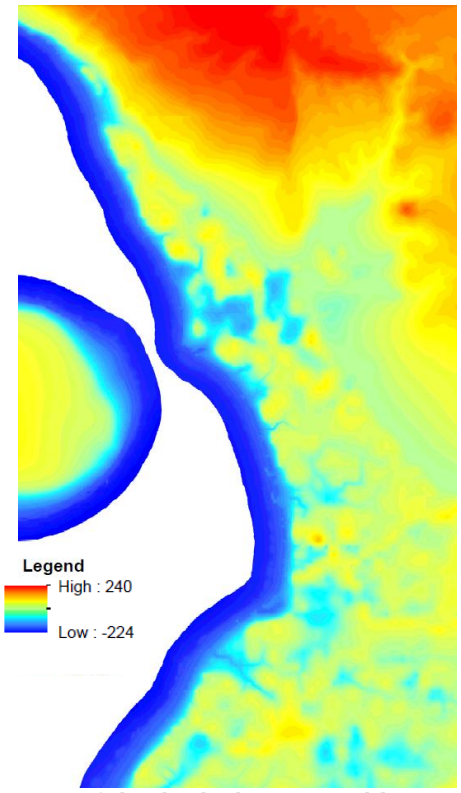

Figure 6. A part of the depth chart, created by ir. H.J. Stuiver (Laboratory of Geo-information Science and Remote Sensing, Wageningen University) with ArcMap. A part of Klein Bonaire is visible on the left and the area of Kralendijk is visible on the right

3.1.2 GoPro pictures

After examining the GoPro pictures, WPTs were identified on substrate type, occurrence of benthic cyanobacterial mats between 30m and 70m depth and the biomass of the mats (Table 5). Figure 7 shows the distribution of the different substrate types along the coast. The major part of the north-west coast is a cliff and a mayor part of the south-west coast contains a flat bottom with rubble. Around Klein Bonaire a lot of flat and sandy bottoms without BCMs are present.

Table 5. Classification of waypoints (WPTs)

Substrate type	Biomass of mats	WPTs	% of total
Flat & sand	High (4)	7	6
	Intermediate (3)	2	2
	Low (2)	4	3
	Very low (1)	19	17
	non	23	20
Flat & rubble	non	27	23
Cliff	non	33	29
Total with BCMs		32	28
Total		115	

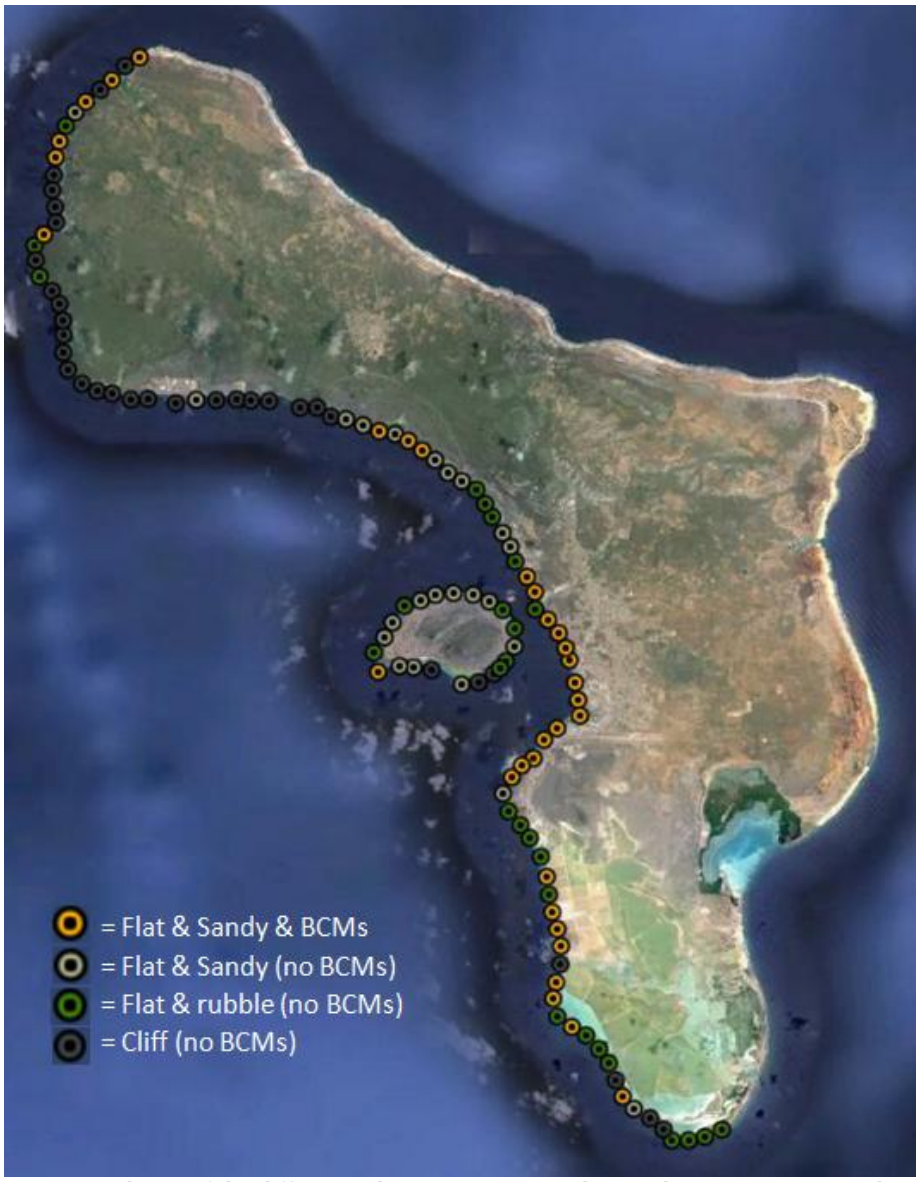

Figure 7. A depict of the different substrate types according to the GoPro pictures taken on the track of each WPT. Different dots indicate different substrate types along the coast

In total BCMs were found at 32 WPTs. Thereof seven WTPs contained a high biomass of mats, all in front of the city Kralendijk (Figure 8). Furthermore, benthic cyanobacterial mats containing very low biomass were also found on the north-west coast (Washington Slagbaai National Park) and south-west coast (Salt lakes). BCMs were only found on a relative flat and sandy bottom.

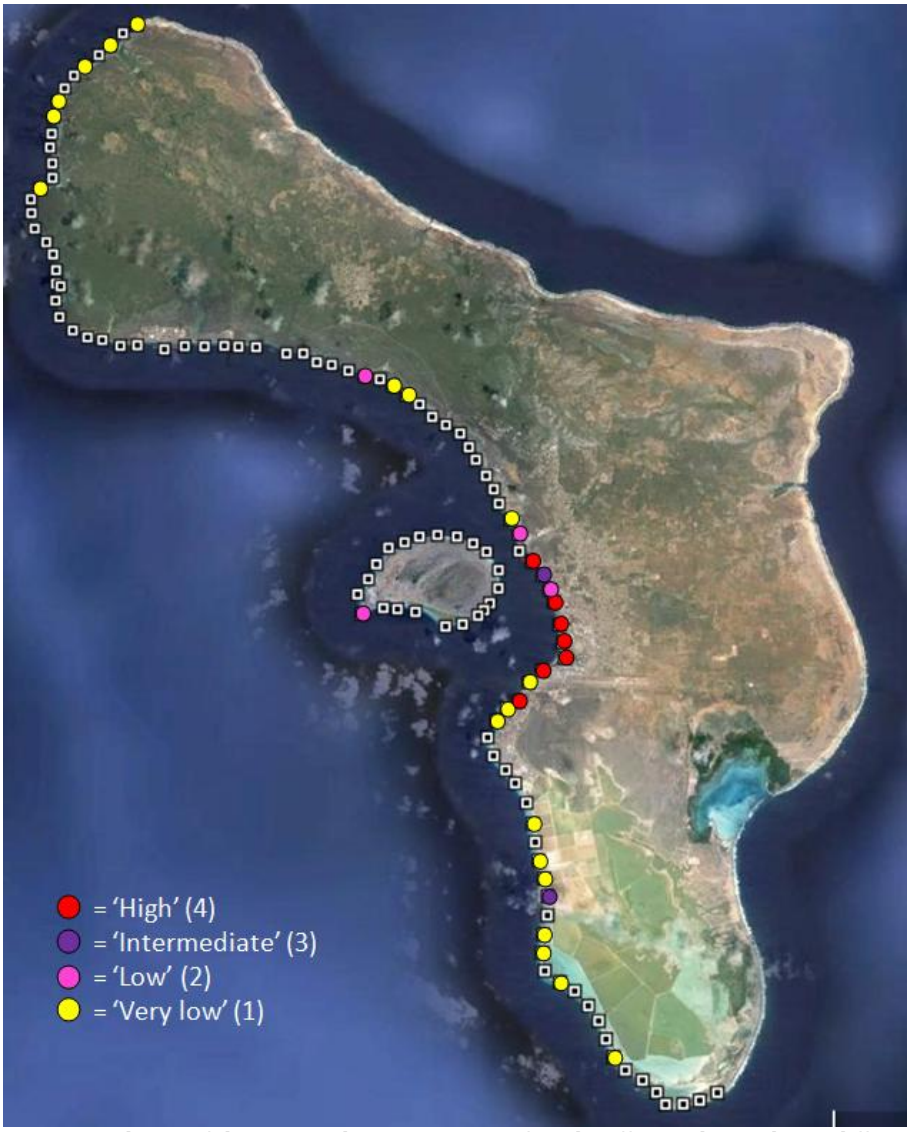

Figure 8. A depict of the WPTs where BCMs were found. Different dots indicate different biomass of the mats (See Table 1)

Nine WPTs containing benthic cyanobacterial mats ('cyano waypoints'), were chosen to be used for the BCMs characterisation study. Three waypoints containing no benthic cyanobacterial mats ('no-cyano/control waypoints'), were chosen as control samples. Since BCMs only occurred on a relative flat and sandy bottom, control WPTs were chosen to contain also a relative flat and sandy bottom, to try to minimize the abiotic differences between the control and the cyano WPTs. All 12 WPTs were spread on the central west coast of Bonaire and Klein Bonaire (Figure 9).

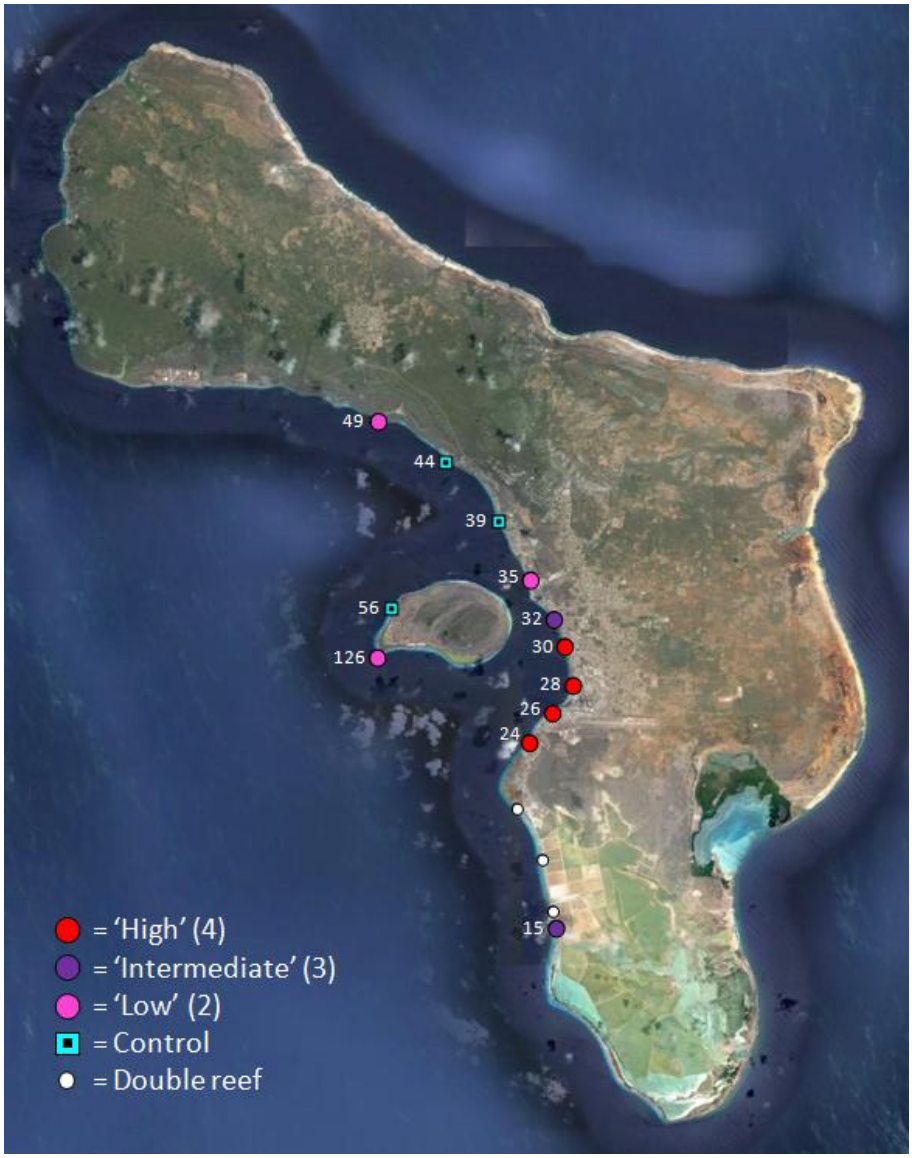

Figure 9. A depict of the WPTs chosen for BCMs characterisation study. Different dots indicate the different WPT types and biomass of the mats (See Table 1)

3.2 Results – BCMs characterisation study

3.2.1 Habitat conditions

Figure 10 shows the measured habitat conditions per sample depth, averaged from the two measurements closest to the sample depth. Overall there is more variation in the deep measurements (C10/D0/D5) than in the shallow measurements (S0/S5), excepts for the PAR relative to the surface light (relative_PAR). As main differences it seems that the pH is lower at the control measurement (C10), the (relative) PAR is lower at the deep measurements (C10/D0/D5) and the chlorophyll is lower at the shallow measurements (S0/S5).

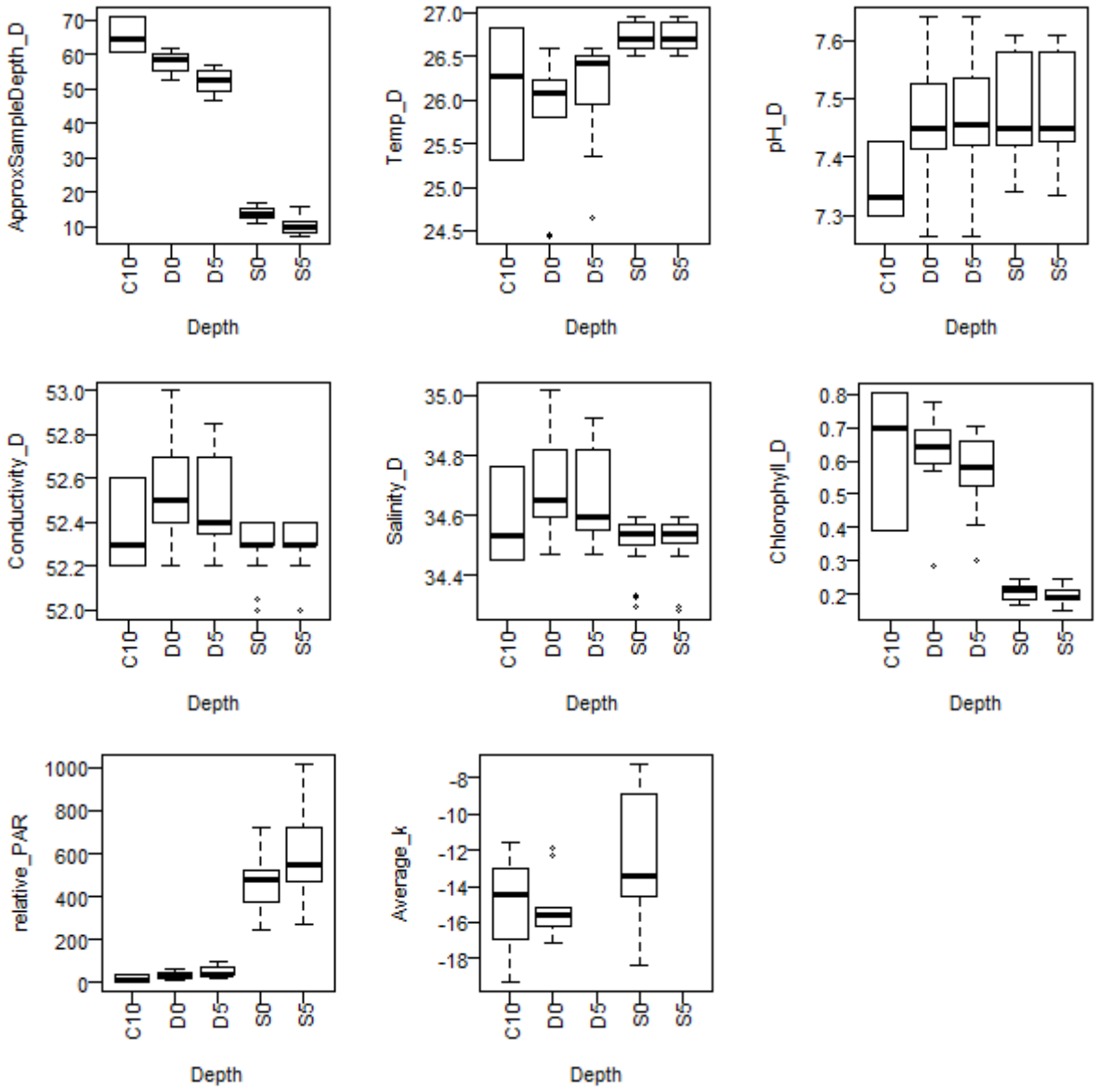

Figure 10. Boxplots of measured habitat conditions. The two measurements closest to the sample depth were averaged and used for the analysis. C10 = control sample, D0 = deep measurement 0m above the BCM, D5 = deep measurement 5m above the BCM, S0 = shallow measurement 0m above the BCM, S5 = shallow measurement 5m above the BCM. N: C10=3, D0=9, S0=9

3.2.2 Light availability

In Figure 11 the light intensity at different depths relative to the surface light is shown, in which the solid line depicts the deep deployment and the dashed line depicts the shallow deployment. On average the deepest measurement of the deep deployment was at 61.43m and the deepest measurement of the shallow deployment was at 16.61m (Table 7). The relative light intensity remaining at the different depths differs per WPT and between the deep and shallow deployment (Appendix, p38). Despite these difference, it does stand out that at 3,7m depth less than 40% of the surface light intensity in the red spectra (>610nm) is left and around 14.5m depth almost no red light is left (Figure 11).

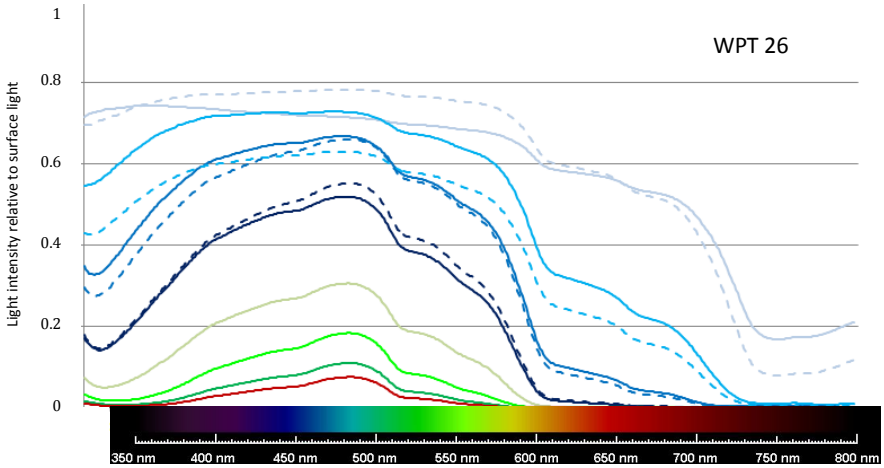

Figure 11. A graph of the relative light intensity data. All data was calculated relative to the first under-water measurement and grouped per certain depths (Table 6). Solid line = deep measurement, dashed line = shallow measurement

Table 6. Upper and lower measurement boundary (m) of the depth grouping, indicated by colours

< 2
>2 – 5,5
5,5 – 10
10 – 20
20 – 30
30 – 45
45 – 55
60 – 65 (Deepest)

Table 7. Overall average depth (m) per measurement grouping

Deep	Shallow
1.40	1.41
3.69	3.79
7.82	7.81
14.67	13.88
25.24	
40.28	
52.94	
61.43	

Table 8 shows the wavelength with the highest intensity at the deepest measurement. For the deepest measurement of the deep deployment this ranges between 483nm and 489nm, for the deepest measurement of the shallow deployment this ranges between 482nm and 485nm (Figure 12). The wavelength with the highest intensity at the deepest measurement at the control WPT ranges between 486nm and 492nm. On average 5% of the light intensity ranges between 463nm and 500nm, calculated from the measurements of the deep deployment (Table 8).

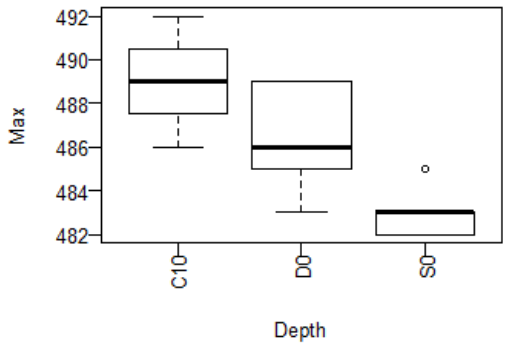

Figure 12. A boxplot on the wavelengths of the maximum light intensity of the deepest measurements. Means: C10=489, D0=486.4, S0=483.1. N: C10=3, D0=9, S0=9

Table 8. The table below shows the wavelength with the maximum light intensity at the deepest measurement. Also the wavelength of 1% / 5% / 33% light intensity are shown. Actual depth of measurement can be found in the right column

	Max at 61m	>1% lower limit	>1% upper limit	>5% lower limit	>5% upper limit	Depth
WPT15D	485	379	538	479	488	60.39
WPT24D	489	379	548	458	503	60.24
WPT26D	483	372	552	443	505	59.82
WPT28D	486	375	545	476	492	60.45
WPT30D	486	369	556	465	500	60.17
WPT32D	489	374	563	446	510	62.97
WPT35D	489	378	552	465	502	62.66
WPT49D	485	377	547	458	502	63.31
WPT126D	486	384	546	473	496	62.83

	Max at 16m	>33% lower limit	>33% upper limit	>45% lower limit	>45% upper limit	Depth
WPT15S	482	388	514	462	494	16.60
WPT24S	482	397	510			16.25
WPT26S	485	394	527	462	498	16.64
WPT28S	485	358	573	375	551	15.99
WPT30S	482	380	519	462	493	16.01
WPT32S	483	361	565	382	539	17.17
WPT35S	483					17.29
WPT49S	483	388	526	467	495	16.19
WPT126S	483	380	543	419	509	17.31

	Max at 61m	>1% lower limit	>1% upper limit	>5% lower limit	>5% upper limit	Depth
CWPT39	492	422	534			62.88
CWPT44	489	385	550			62.53
CWPT56	486	369	557	435	507	59.99

3.2.3 Phycobilisomes – Hydrophilic pigments

During the AMINCO procedure it was noted that the samples obtained different colours, ranging from yellow, orange, pink to purple (Figure 13).

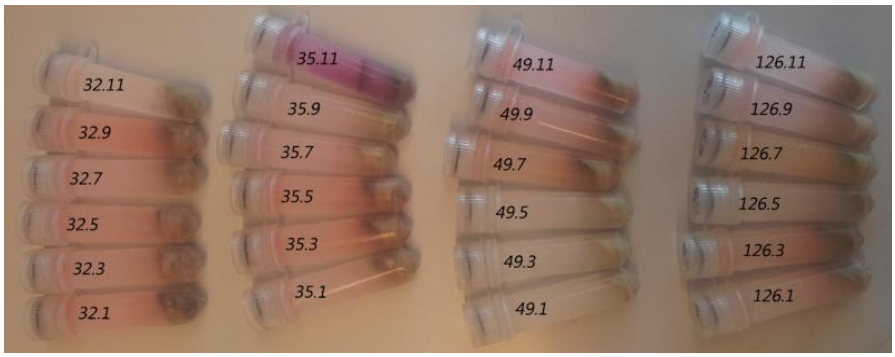

Figure 13. Picture taken after the AMINCO analysis

Figure 14 shows the absorption per 100 g AFDW of two WPTs. It can be noted that the amount of absorption differs per WPT, where sometimes the shallow samples have the highest absorption, sometimes the deep samples have the highest absorption and sometimes there is no consistency. Absorption peaks can be found around 494nm, 540nm and in some samples a small peak is found around 672nm, originating from phycoerythrin (494nm and 540nm) and allophycocyanin (672nm). Furthermore in some samples a shoulder is found on the right side of the 540nm peak, which could indicate another phycoerythrin peak. It is remarkable that no phycocyanin peak (624nm) was found (Figure 14).

Figure 15 shows the wavelengths of the maximum light absorption of peak 1, 2 and the APC peak. The boxplot on peak 1 shows a possible difference between the average of deep and shallow samples.

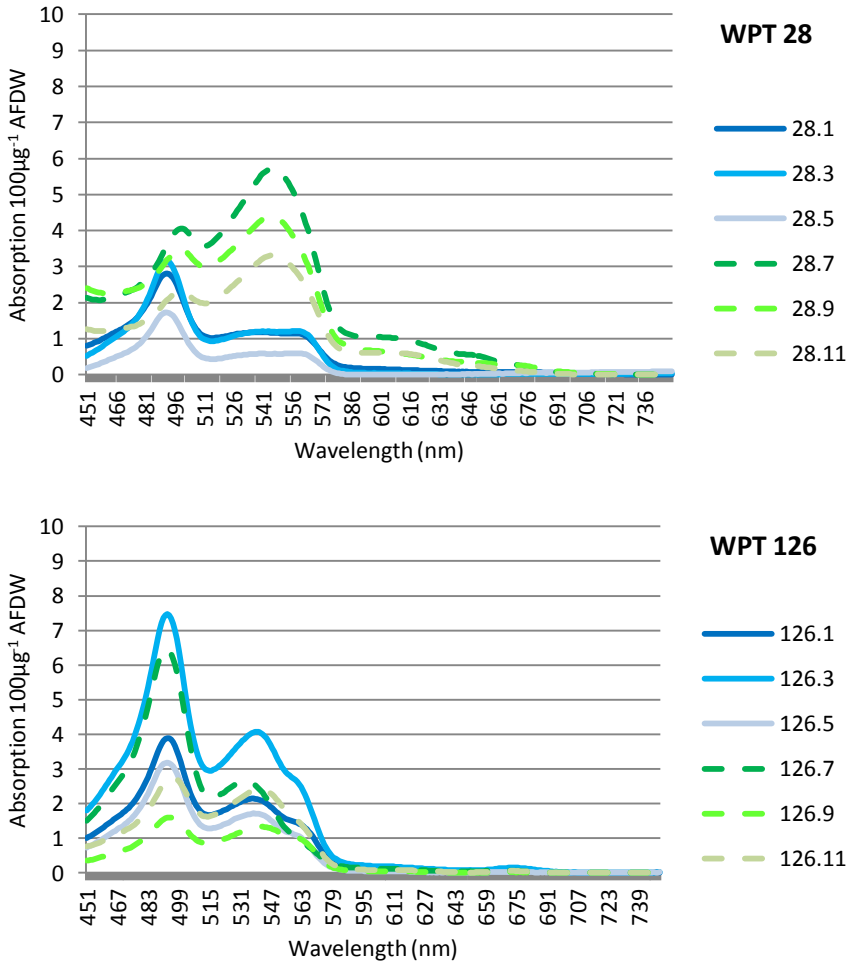

Figure 14. Two examples of the absorption spectra per 100µg AFDW. Each sample is normalized on their lowest absorption point. x.1/x.3/x.5 are deep samples, x.7/x.9/x.11 are shallow samples

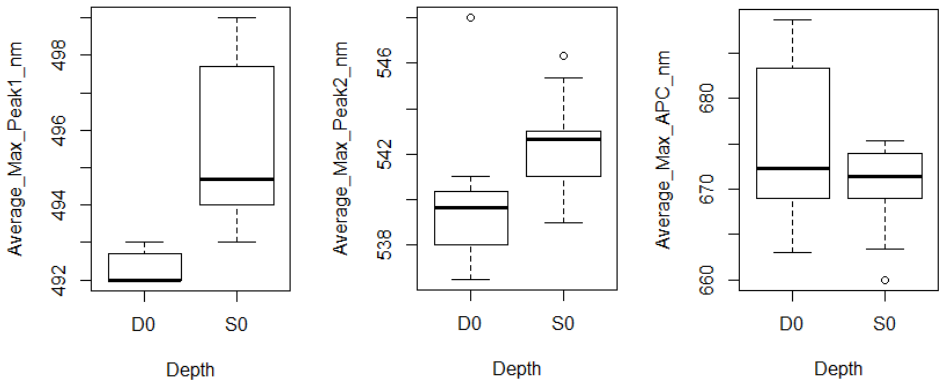

Figure 15. A boxplot on the wavelengths of the maximum light absorption of peak 1, 2 and APC peak, shown per sample and depth. n=9

3.2.4 Hydrophobic pigments

In total twelve pigments were found (Table 9). On average, in shallow samples chlorophyll a, zeaxanthin and fucoxanthin are present in the highest amount, in deep samples chlorophyll a,

fucoxanthin and chlorophyll b are present in the highest amount. In the shallow samples alloxanthin, violaxanthin and chlorophyll c3 are present in the lowest amount. In the deep samples, violaxanthin, diatoxanthin and alloxanthin are present in the lowest amount. Thereof violaxanthin is found in 23% of the deep samples (6/26), and diatoxanthin and alloxanthin are both present in only one deep sample. The other pigments are present in all 54 samples (Table 9).

Table 9. The twelve different pigments found in the sample. The average amount per pigment in shallow and deep samples is shown. Dark grey = highest amount, light grey = lowest amount, green = light protecting pigment, blue = higher amount in deep samples

		S0		D0	
Pigment	**Abbreviation**	**mg pigment/ g AFDW**	**% of total pigment**	**mg pigment/ g AFDW**	**% of total pigment**
Chlorophyll a	Chla	2.826	75.39	4.163	82.55
Zeaxanthin	Zeax	0.277	7.40	0.106	2.10
Fucoxanthin	Fuco	0.226	6.03	0.398	7.89
Diadinoxanthin	Diad	0.148	3.94	0.019	0.38
Chlorophyll c2	Chlc2	0.076	2.02	0.089	1.77
Chlorophyll b	Chlb	0.054	1.43	0.123	2.43
B Carotene	Bcar	0.037	0.99	0.029	0.57
Peridinin	Peri	0.034	0.92	0.018	0.36
Diatoxanthin	Diat	0.032	0.85	0.001	0.01
Alloxanthin	Allo	0.027	0.71	0.001	0.01
Chlorophyll c3	Chlc3	0.010	0.26	0.089	1.76
Violaxanthin	Viol	0.003	0.07	0.008	0.17
Total		3.749		5.043	

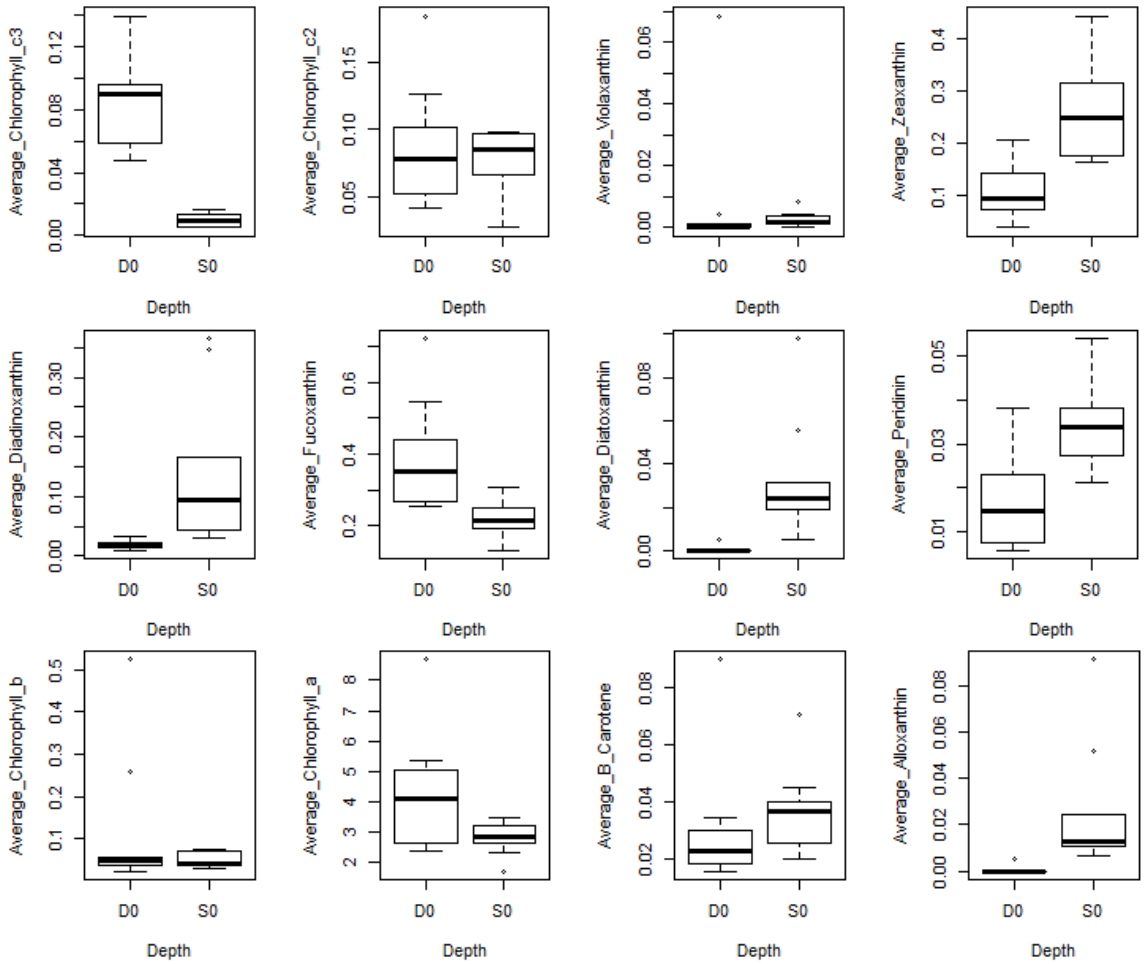

Figure 16. Boxplots of the pigments found. N: D0=9, S0=9

When looking at the boxplots shown per pigment, a trend of differences in means is visible, indicating that there might be differences between the means of deep and shallow samples per pigment (Figure 16). After a log-transformation, a significant difference between the total amount of pigments in deep and shallow samples was found (p=0.005, Figure 17 A, B). A significant interaction between depth and WPT is found for most pigments, therefore being unable to draw conclusion on the influence on depth or WPT of most of the pigments (Table 10). However, no significant interaction between depth and WPT was found for chlorophyll c3 and zeaxanthin. After a square root transformation chlorophyll c3 showed a significant effect of both depth ($p < 2.20^{-16}$) and WPT ($p = 0.0004$), with more chlorophyll c3 in deep samples (Table 10, Figure 17). After a log10 transformation zeaxanthin showed a significant effect of depth ($p = 4.62^{-8}$), with less zeaxanthin in deep samples.

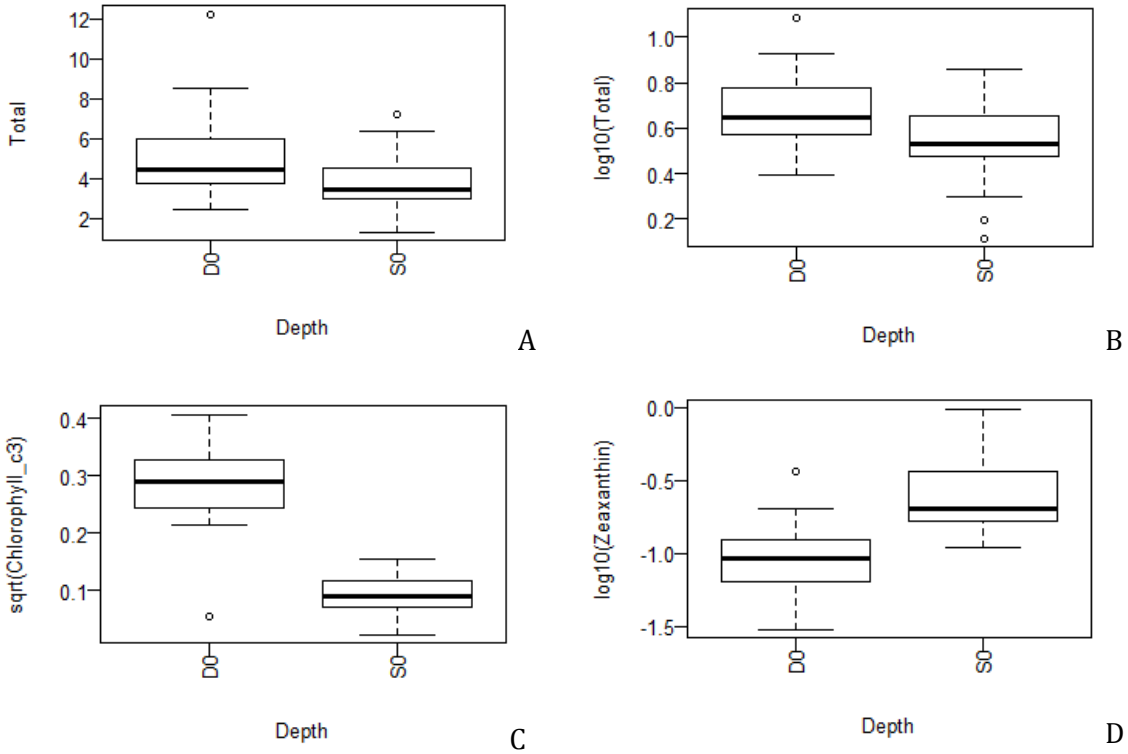

Figure 17. Boxplots on the total amount of pigments (A = Non-transformed data, B = Log transformed data, n=27) and boxplots on the pigments with a significant difference between depths (C = sqrt transformed chlorophyll c3 data, D = log10 transformed zeaxanthin data, n=9)

Table 10. Overview of the statistical analysis on the pigment data and the outcome

			Two-way ANOVA					
			P value					
Data	Zero -values	Transformation	Interaction		P value Depth		P value WPT	
Chlorophyll_c3	N	sqrt	0.157731		2.2E-16	***	0.000294	***
Chlorophyll_c2	N	No	0.000113	***	0.045017	*	8.47E-06	***
Violaxanthin	Y (34)	-	-		-		-	
Zeaxanthin	N	Log10	0.06356	.	1.8E-05	***	0.05378	.
Diadinoxanthin	N	Log10	0.000298	***	2.49E-11	***	0.08636	.
Fucoxanthin	N	sqrt	0.004345	**	3.55E-08	***	0.000565	***
Diatoxanthin	Y (26)	-	-		-		-	
Peridinin	N (2)	No	0.000257	***	1.19E-07	***	0.001657	**
Chlorophyll_b	N	log10	7.08E-06	***	0.009017	**	1.14E-07	***
Chlorophyll_a	N	sqrt	0.03266	*	0.000772	***	0.032182	*
B_Carotene	N	log10	0.001358	**	0.042508	*	0.442007	
Alloxanthin	Y (31)	-	-		-		-	

4.1 Discussion – BCMs distribution study

During the distribution study the aim was to survey the distribution of the benthic cyanobacterial mats along the west coast of Bonaire, including the island 'Klein Bonaire', between 30 and 70 meters depth. Almost 30% of the Bonairean west coast contained deep BCMs (Table 5). In Figure 7 it is noticeable that thereof 44% is in front of Kralendijk or its suburbs along the coast (14 WPTs). Moreover, all benthic cyanobacterial mats with a high biomass occur in front of the city Kralendijk and there are only three spots outside of this urban area containing BCM with 'low'/'intermediate' biomass (Figure 8). The remaining 15 WPTs contain 'very low' biomass and thereof eight WPTs are in front of the salt lakes. The higher occurrence of BCMs close to urbanized areas has also been found on shallow reefs of Curacao by Brocke et al. (2015). This might indicate that extensive growth of deep BCMs on Bonaire is related to anthropogenic activities, causing for instance nutrient enrichment. The stimulation of cyanobacterial growth by nutrient enrichment is noted by for instance Paerl et al. (2011) and O'Neil et al. (2012) and anthropogenic pressure on the Bonairean coast has already been documented before (Debrot et al., 2013; Govers et al., 2014; Slijkerman et al., 2014).

However, during the distribution study it was also noted that benthic cyanobacterial mats only occurred on a sandy and relative flat ocean floor (Table 5). According to the GoPro pictures, 29% of the inspected Bonairean west coast is a cliff, resulting in steep underwater coastal areas that do not flatten out before reaching 100m depth. This is mostly seen on the north-west coast of Bonaire and explains why almost no benthic cyanobacterial mats were found there (Figure 7). Plate forming limestone and old corals dominate the steep coast. Possibly these substrates do not offer enough grip for the cyanobacteria to settle on and form mats. About 23% of the Bonairean west coast flattens out around 45 meters depth, but does contain rubble and also here no benthic cyanobacterial mats were found. It could be that the rubble attracts other organisms, including herbivorous fish, what the development of BCMs prevents. The remaining 20% of the WPTs contain a flat and sandy bottom, but did not contain cyanobacterial mats. Possibly a flat and sandy bottom is a key requirement for a benthic cyanobacterial mats to develop, therefore excluding 52% of the Bonairean west coast. But not all flat and sandy bottoms are covered with BCMs, what indicated that there are other conditions that might be required as well. As stated before, rather than only one factor, multiple factors need to be favourable simultaneously to stimulate excessive proliferation of cyanobacteria (Paerl et al., 1985; Heisler et al., 2008). Considering the distribution of deep BCMs it is most likely that pollution, associated with the most densely populated coast of Bonaire, namely Kralendijk, plays a role. Further research should investigate how big the effect is of pollution, originating from urbanized areas, on BCMs formation and if this factor can be minimized.

4.2 Discussion – BCMs characterisation study

4.2.1 Habitat conditions

There are a few notable differences found in the data on the habitat conditions. Bak et al. (2005) stated that deep reefs encounter 'limited influence of fluctuations in major factors' and that they are 'connected to the more resilient environment of the deeper ocean'. This is not in line with the measurements presented here. It seems that the shallow reef provides a more stable environment than the deep reef, since overall there is less variation in the shallow measurements. However, there is quite some variation in the control samples (C10), which indicates that other unknown factors might have influenced the measurements in this study, indicating that more measurements are needed to get a better overview of the habitat conditions.

4.2.2 Light availability

To describe and compare the light availability at the deep and shallow BCM locations, the measurements were averaged per depth group and transformed relative to the surface light.

However, there is a lot of variation in the average light intensity, as well per depth group, as between WPTs, as between the same depths on deep and shallow deployments. Nevertheless, some observations were made.
On the right hand side of the peak the light intensity decreases with steps (Figure 11). At all twelve WPTs light of 730nm and more is already filtered out at 3.7m depth, light of 600nm and more is almost completely filtered out at 14.5m depth and at a depth of 61.4m less than 5% is left of the light intensity of 510nm and more. This means that photosynthetic organisms living in less than 15m water depth could get energy of wavelengths above 600nm, although less than 40% intensity remains below 3.7m depth. Photosynthetic organisms living around 61.4m depth probably get most energy of wavelengths between 463nm and 500nm, since only here more than 5% light intensity is left.

4.2.3 Phycobilisomes – Hydrophilic pigments

Already during the sample analysis differences in colour indicated that the pigments in the samples differed (Figure 13). Not only did the intensity of colour differ, what indicates difference in the amount of pigment, also the colour itself differed, what indicates there are differences in the type of pigments. These differences in colour were also found by Six et al., (2007).
When looking at the absorption graphs indeed a lot of differences are found (Figure 14; Appendix, p44). Firstly, the level of absorption differs between WPTs and replicates. The highest peak height ranges from 0.5 and 9.5 absorption 100 g^{-1} AFDW. Secondly, there is no uniformity on the differences between absorption of deep and shallow samples per WPT. At some WPTs more absorption occurs in deep samples, at some WPTs more absorption occurs in shallow samples and sometimes it differs per replicate. Thirdly, the pattern within the shallow samples is not the same. In deep samples peak 1 is always the highest peak, but in shallow samples sometimes peak 2 is the highest peak. Therefore no conclusions can be drawn on the differences between the level of absorption in shallow and deep samples.
Most of the samples show a clear peak around 494nm (peak 1) and around 540nm (peak 2) (Figure 14). These peaks are respectively PUB and PEB peaks (Grossman et al., 1993). Also the shoulder on the right side of peak 2 is thought to originate from PEB. However, calculations on the amount of phycobilisomes are performed by a formula from Beer & Eshel (1985), which has lately been revised by Sampath-Wiley & Neefus (2007) into a more accurate formula. To calculate the amount of PE these methods make use of a clear peak around 564nm and to calculate the amount of PC a peak around 624nm is used (Sampath-Wiley & Neefus, 2007). In this research only a shoulder is found around 564nm and only in some samples. Therefore calculations on the amount of absorption on these samples would be highly inaccurate. Moreover, a peak around 624nm is absent. This means that no PC was detected in the samples, but it is known that PC is always present in a phycobilisomes molecule/structure, because PC is at the base of this molecule (MacColl, 1998). A peak around 650nm was also absent, indicating that no APC was detected. Again, this molecule is at the base of a phycobilisomes molecule and therefore cannot be missing. This makes the performed analyses questionable. It would be interesting to perform the analyses again to compare the results, and at the same time use another method to detect PC and APC.
When comparing the available light (Table 8) to the phycobilisomes found (Figure 15), it shows that the PUB absorption peak falls within the 5% light intensity range. Also, normally the 564nm PEB peak is clearer than the 534nm PEB peak, but here it is the other way around. This could indicate that these benthic cyanobacterial mats were subjected to photo acclimatisation and therefore have more antennas in the blue-green spectra and less in the yellow-red spectra, so that they can survive in deeper waters.

4.2.4 Hydrophobic pigments

The twelve pigments found in the samples are originating from different organisms, like chlorophytes, diatoms and dinoflagellates, including zeaxanthin, originating from cyanobacteria,

showing that indeed different organisms form a consortium in these mats (Bianchi et al., 2000; Rejmánková & Komárková, 2000; Schlüter et al., 2006; Charpy et al., 2012).
On average deep samples contained more pigments than shallow samples (p=0.005)(Figure 17). Although it could not be statistically proved, this was mainly caused by the difference in the amount of chlorophyll a (Table 9). Only for chlorophyll c3 and zeaxanthin no significant interaction between depth and WPT were found, meaning that some conclusions on the effect of depth can be drawn (Table 10). Deep samples contained on average 47% more chlorophyll c3 than shallow samples, what could contribute to the amount of energy taken up, since chlorophyll c3 is a light absorption pigments (Grossman et al., 1993). This is according to the expectations, since organisms on the deep reef need more light absorption pigments to gain the same amount of energy as organisms on the shallow reef. Deep samples did also contain on average 62% less zeaxanthin, a light protecting pigment (MacIntyre et al., 2002; Schlüter et al., 2006). This is also according to the expectations, because organisms on the deep reef are subjected to less photo oxidation than organisms on the shallow reef (Eloff et al., 1976).
Because of the significant interaction between depth and WPT for the remaining pigments, what means that their effects cannot be separated, only some interpretations can be made on their account. It is interesting that, although not significant, zeaxanthin, diadinoxanthin, B-Carotene and diatoxanthin, which are all light protecting pigments, have an higher average in shallow samples (Table 11)(MacIntyre et al., 2002; Schlüter et al., 2006). All four different types of chlorophyll, which are light absorption pigments, have a higher average in deep samples (Table 11)(Grossman et al., 1993). Therefore it would be interesting to repeat this part of the research with a higher sample size, to increase the possibility of significant differences.
It is also notable that violaxanthin, diatoxanthin and alloxanthin are only present in few of the deep samples. This could indicate that the deep samples are contaminated with shallow sample material.

Table 11. An overview of the twelve found pigments, the organisms they origin from and their function. The pigments in grey have a higher average in deep samples. 1= Schlüter et al., 2006, 2= de Boer et al., 2015, 3= Wright, 1991, 4= MacIntyre et al., 2002, 5= Haxo & Blinks, 1950, 6= Grossman et al., 1993, 7= Hewes et al., 1998, 8= Cruz & Serôdio, 2008, 9= McConnell et al., 2002

Pigment	Organisms	Ref	Function	Ref
Chlorophyll a	non specific	3, 9	light absorption	6
Zeaxanthin	Cyanobacteria	1, 2	light protecting pigments	1, 4
Fucoxanthin	Diatoms (Chrysophytes)	1, 3, 5, 7	light absorption	5
Diadinoxanthin	Diatoms, Dinoflagellates, Euglenophyte	1, 8	light protecting pigments	1
Chlorophyll c2	Cryptophytes	1	light absorption	6
Chlorophyll b	Chlorophytes, Euglenophyte	1, 3	light absorption	6
B Carotene	Non specific	2	light protecting pigments	1, 4
Peridinin	Dinoflagellates	1, 3, 7	light absorption	6
Diatoxanthin	Diatoms	2, 8	light protecting pigments	1
Alloxanthin	Cryptophytes (1), Cryptomonads (3)			
Chlorophyll c3	Chrysophytes	1, 7	light absorption	6
Violaxanthin	Cryptophytes	3	increases in reduced light (1), non quenching (4)	

4.3 Discussion – Field observations

While diving and sampling, some remarkable observations were made.
The WPTs used for the BCMs characterisation study were selected based on the classification in Table 1. However, the quality of the BCMs found during the deep sampling dives did not always correspond to this. While at a WPT it was expected to find substantial mats, the BCMs were experienced as thin and incoherent, and vice versa. This indicates that the GoPro pictures taken per WPT during the distribution study, as well as the footage taken by the underwater camera, do not represent the state of the deep BCMs while performing the sampling dives, which may be due to various reasons. First of all it might be that the quality of a BCM cannot be judged from the appearance of the mat on a picture. On a picture a mat might appear to be dense, but in reality have a loose structure. Also, although a field stretches from 45 until at least 60 meters

depth and often stretches as far as one can see, the field might not be homogeneous. The GoPro pictures cover only a small area and therefore the pictures might not represent the quality of the whole field. If this true, then the BCMs on the GoPro pictures do not correspondent with the BCMs that are sampled by the deep divers. In addition, it is highly unlikely that the deep divers sample at the exact location of where the GoPro pictures were taken. It could also be that the structure of BCMs change as a response to diurnal variations in the light intensity. Since the GoPro pictures on different WPTs were taken at various time points, BCMs might be captured in different 'stages' of quality. All deep dives were performed between 9:04 and 9:58, which might be 'the wrong time of the day'. It might also be that BCMs are able to change because of other factors, but more research is needed on this. Overall it could be concluded that a better estimation of the quality of the BCMs (at the moment of sampling) is obtained by inspecting them during a dive instead of capturing them on tape.

It was also noted that the deep cyano-fields appeared to be overall of the same consortium. On the shallow reef, different consortiums of cyanobacteria, algae and macroalgae are present (Charpy et al., 2012). The shallow samples were taken from sandy patches between corals, because it was thought that this would correspond with the deep BCMs, which were only found on sandy and flat bottoms. Nonetheless, differences in thickness and structure (sliminess) between shallow samples were noted during the sampling procedure. Overall the shallow BCMs were highly interwoven and contained a dense structure, and were therefore easy to sample. The deep BCMs contained a very loose structure and low density, and were therefore hard to sample.

Besides these difference in quality between BCMs on GoPro pictures and sampled BCMs, and deep and shallow BCMs samples, another observation was made. In the materials and methods section (Figure 5) and in the results section on the WPT selection (Figure 9), three WPTs on the double reef were pointed out as well. It was planned to take samples from the double reef, but this appeared not possible, since the BCMs did disappear between the distribution study and the characterisation study. Although pictures were taken of these BCMs (20-4-2015) and they were even seen during recreational dives on these spots, they were no longer present when the sampling dives were conducted (7-5-2015). To exclude the possibility that this was due to diurnal rhythms, multiple dives were preformed during the day. During the dives intended to sample the BCMs, it was noted that, in contrast to the former preformed recreational dives, garden eels were present. It is not known if the BCMs did disappear because of the appearance of the garden eels, or that the garden eels did settle at these spots because BCMs were not present anymore. No further fieldwork has been performed on the disappearance of the BCMs and the appearance of the garden eels.

5.1 Conclusions

During this research, first a BCMs distribution study was performed on the west coast of Bonaire, to map the appearance of benthic cyanobacterial mats (BCM) between 30 and 70 meters depth. Almost 30% of the Bonairean west coast (32 WPTs) contained cyanobacterial mats. Thereof 44% were in front of Kralendijk or its suburbs along the coast (14 WPTs). Benthic cyanobacterial mats were only found on a relative flat and sandy ocean floor. This could indicate that a flat and sandy ocean floor are key requirements for a BCM to develop, therefore excluding 53% of the Bonairean west coast. But since not all flat and sandy bottoms are covered with BCMs, other factors, such as pollution associated with the most densely populated coast of Bonaire, namely Kralendijk, probably play a role. More research is needed to investigate how big the effect of pollution on BCMs formation is and if this factor can be minimized. Nine waypoints containing benthic cyanobacterial mats were chosen to be used for the BCMs characterisation study.

During the BCMs characterisation study, multiple aspects were analysed. Hereby, the focus was on the light availability on the deep reef and the light-harvesting pigments of BCMs.

Despite the high variations in the average light intensity, as well per depth group, as between WPTs, as between the same depths on deep and shallow deployments, some observations were

made. At all WPTs light of 730nm and more was already filtered out at 3.7m depth, light of 600nm and more was almost completely filtered out at 14.5m depth and at a depth of 61.4m less than 5% was left of the light intensity of 510nm and more. Therefore photosynthetic organisms living around 61.4m depth probably get most energy of wavelengths between 463nm and 500nm.

To get more insight in the possible photo acclimatisation to the light availability on the deep reef, the following research question was stated: 'What are the differences in the amount and/or the composition of the phycobilisomes between deep and shallow cyanobacterial mats?'. There was no consistency in the amount of absorption and the amount of phycobilisomes per sample depth or WPT. Therefore no conclusion could be drawn on the amount and the composition of the phycobilisomes in deep and shallow BCMs. A clear PUB peak was found around 494nm and a clear PEB peak was found around 540nm. However, no clear peak was found around 564nm, 624nm and 650nm, respectively a PEB, PC and APC peak. Especially the PC and APC peaks are supposed to be detectable, therefore the performed analyses is questioned. It would be interesting to perform the analyses again to compare the results, and at the same time use another method to detect PC and APC.

Besides the phycobilisomes, also hydrophobic pigments were analysed to answer the research question 'What are the differences in the amount and/or composition of the hydrophobic pigments between deep and shallow cyanobacterial mats?'. Twelve pigments were found, including zeaxanthin, which originates from cyanobacteria. According to the expectations, deep samples contained more pigments than shallow samples ($p=0.005$). Deep samples contained on average 47% more of the light absorbing pigment chlorophyll c3 than shallow samples ($p< 2.20^{-16}$), what could contribute to the amount of energy taken up. Deep samples did also contain on average 62% less of the light protecting pigment zeaxanthin ($p=4.62^{-8}$). Although not significant different, zeaxanthin, diadinoxanthin, B-Carotene and diatoxanthin, which are all light protecting pigments, had a higher average in shallow samples than in deep samples. This was also according to expectations, because less photo oxidation occurs at lower light availability. It would be interesting to repeat this part of the research with a higher sample size, to increase the possibility of significant differences and confirm these results.

Acknowledgements

I want to thank Chris Verstappen and Astrid Jager for their excellent work during the deep dives. I would like to thank Petra Visser (UvA), Erik Meesters (IMARES) and Fleur van Duyl (NIOZ) for their help during this research. I want to thank Pieter Slot (UvA) for his help during the pigment analysis and the other procedures in the laboratory. Special thanks to Klaas Metselaar (WUR), without whom all the samples would not have been transported to the Netherlands. Thanks also go to Dean (Stinapa), for the use of the boat, and to Enchio (Stinapa), for his excellent sailing during the fieldwork. Also a special thanks to Haico van Heuzen, for the cooperation during field- and sampling work.

References

Al-Najjar, M. A. A., D. de Beer, M. Kühl, & L. Polerecky, 2012. Light utilization efficiency in photosynthetic microbial mats. Environmental Microbiology 14: 982–992.

Bak, R. P. M., G. Nieuwland, & E. H. Meesters, 2005. Coral reef crisis in deep and shallow reefs: 30 years of constancy and change in reefs of Curacao and Bonaire. Coral Reefs 24: 475–479.

Becking, L. E., & E. H. W. G. Meesters, 2014. Bonaire Deep Reef Expedition I. .

Beer, S., & a Eshel, 1985. Determining phycoerythrin and phycocyanin concentrations in aqueous crude extracts of red algae. Marine and Freshwater Research 36: 785.

Bianchi, T. S., E. Engelhaupt, P. Westman, T. Andrén, C. Rolff, & R. Elmgren, 2000. Cyanobacterial blooms in the Baltic Sea: Natural or human-induced?. Limnology and Oceanography 45: 716–726.

Brocke, H. J., L. Polerecky, D. de Beer, M. Weber, J. Claudet, & M. M. Nugues, 2015. Organic Matter Degradation Drives Benthic Cyanobacterial Mat Abundance on Caribbean Coral Reefs. Plos One 10: e0125445, http://dx.plos.org/10.1371/journal.pone.0125445.

Charpy, L., B. E. Casareto, M. J. Langlade, & Y. Suzuki, 2012. Cyanobacteria in Coral Reef Ecosystems: A Review. Journal of Marine Biology 2012: 1–9.

Codd, G., S. Bell, K. Kaya, C. Ward, K. Beattie, & J. Metcalf, 1999. Cyanobacterial toxins, exposure routes and human health. European Journal of Phycology 34: 405–415.

Cruz, S., & J. Serôdio, 2008. Relationship of rapid light curves of variable fluorescence to photoacclimation and non-photochemical quenching in a benthic diatom. Aquatic Botany 88: 256–264.

De Boer, E. J., M. I. Velez, K. F. Rijsdijk, P. G. B. de Louw, T. J. Vernimmen, P. M. Visser, R. Tjallingii, & H. Hooghiemstra, 2015. A deadly cocktail: How a drought around 4200 cal. yr BP caused mass mortality events at the infamous “dodo swamp” in Mauritius. The Holocene 1–14, http://hol.sagepub.com/cgi/doi/10.1177/0959683614567886.

Debrot, A. O., J. van Rijn, P. S. Bron, & R. de León, 2013. A baseline assessment of beach debris and tar contamination in Bonaire, Southeastern Caribbean. Marine Pollution Bulletin Elsevier Ltd 71: 325–329, http://dx.doi.org/10.1016/j.marpolbul.2013.01.027.

Eloff, J. N., Y. Steinitz, & M. Shilo, 1976. Photooxidation of cyanobacteria in natural conditions. Applied and environmental microbiology 31: 119–126, http://www.pubmedcentral.nih.gov/articlerender.fcgi?artid=169727&tool=pmcentrez&rendertype=abstract.

Everroad, C., C. Six, F. Partensky, J. C. Thomas, J. Holtzendorff, & a. M. Wood, 2006. Biochemical bases of type IV chromatic adaptation in marine Synechococcus spp. Journal of Bacteriology 188: 3345–3356.

Feitoza, B. M., R. S. Rosa, & L. a Rocha, 2005. Ecology and zoogeography of deep reef fishes in northeastern Brazil. Bull. Mar. Sci. 76: 725–742, <Go to ISI>://000229573700010.

Gantt, E., 1974. Phycobilisomes of Porphyridium cruentum: Pigment Analysis. Biochemistry 13: 2960–2966.

Gantt, E., 1981. Phycobilisomes. Annual Review of Plant Physiology 32: 327–347.

Gardner, T. A., I. M. Côté, J. A. Gill, A. Grant, & A. R. Watkinson, 2003. Long-Term Region-Wide Declines in Caribbean Corals. Science 301: 958–960.

Glibert, P. M., & D. a. Bronk, 1994. Release of dissolved organic nitrogen by marine diazotrophic cyanobacteria, Trichodesmium spp. Applied and Environmental Microbiology 60: 3996–4000.

Glynn, P. W., 1991. Coral reef bleaching in the 1980s and possible connections with global warming. Trends in ecology & evolution (Personal edition) 6: 175–179.

Govers, L. L., L. P. M. Lamers, T. J. Bouma, J. H. F. de Brouwer, & M. M. van Katwijk, 2014. Eutrophication threatens Caribbean seagrasses – An example from Curaçao and Bonaire. Marine Pollution Bulletin Elsevier Ltd 89: 481–486, http://linkinghub.elsevier.com/retrieve/pii/S0025326X14005955.

Grossman, A. R., M. R. Schaefer, G. G. Chiang, & J. L. Collier, 1993. The phycobilisome, a light-harvesting complex responsive to environmental conditions. Microbiological reviews 57: 725–749.

Hallock, P., 2005. Global change and modern coral reefs: New opportunities to understand shallow-water carbonate depositional processes. Sedimentary Geology 175: 19–33, http://linkinghub.elsevier.com/retrieve/pii/S0037073805000515.

Haxo, F. T., & L. R. Blinks, 1950. Photosynthetic action spectra of marine algae. The Journal of general physiology 33: 389–422.

Heisler, J., P. M. Glibert, J. M. Burkholder, D. M. Anderson, W. Cochlan, W. C. Dennison, Q. Dortch, C. J. Gobler, C. a. Heil, E. Humphries, a. Lewitus, R. Magnien, H. G. Marshall, K. Sellner, D. a. Stockwell, D. K. Stoecker, & M. Suddleson, 2008. Eutrophication and harmful algal blooms: A scientific consensus. Harmful Algae 8: 3–13.

Hewes, C. D., B. G. Mitchell, T. a. Moisan, M. Vernet, & F. M. H. Reid, 1998. The Phycobilin Signatures of Chloroplasts From Three Dinoflagellate Species: a Microanalytical Study of Dinophysis Caudata, D. Fortii, and D. Acuminata (Dinophysiales, Dinophyceae). Journal of Phycology 34: 945–951, http://doi.wiley.com/10.1046/j.1529-8817.1998.340945.x.

Kramer, P. A., 2003. Synthesis of Coral Reef Health Indicators for the Western Atlantic: Results of the AGRRA Program (1997-2000). Status of Coral Reefs in the western Atlantic: Results of initial Surveys, Atlantic and Gulf Rapid Reef Assessment (AGRRA) Program Research Bulletin 496. .

Leão, P. N., N. Engene, A. Antunes, W. H. Gerwick, & V. Vasconcelos, 2012. The chemical ecology of cyanobacteria. Natural Product Reports 29: 372.

Lesser, M. P., & J. H. Farrell, 2004. Exposure to solar radiation increases damage to both host tissues and algal symbionts of corals during thermal stress. Coral Reefs 23: 367–377.

Lesser, M. P., M. Slattery, & J. J. Leichter, 2009. Ecology of mesophotic coral reefs. Journal of Experimental Marine Biology and Ecology Elsevier B.V. 375: 1–8, http://dx.doi.org/10.1016/j.jembe.2009.05.009.

MacColl, R., 1998. Cyanobacterial phycobilisomes. Journal of structural biology 124: 311–334, http://www.ncbi.nlm.nih.gov/pubmed/10049814.

MacIntyre, H. L., T. M. Kana, T. Anning, & R. J. Geider, 2002. Photoacclimation of photosynthesis irradiance response curves and photosynthetic pigments in microalgae and cyanobacteria. Journal of Phycology 38: 17–38.

McConnell, M. D., R. Koop, S. Vasil'ev, & D. Bruce, 2002. Regulation of the distribution of chlorophyll and phycobilin-absorbed excitation energy in cyanobacteria. A structure-based model for the light state transition. Plant physiology 130: 1201–1212.

Meltvedt, A., & C. Jadot, 2014. Progression of the Coral-Algal Phase Shift in the Caribbean : A Case Study in Bonaire, Dutch Caribbean. Marine Technology Society Jouranl 48: 33–41.

NOAA, 2008. Science expedition to coral reefs in Caribbean helps launch International Year of the Reef. http://www.noaanews.noaa.gov/stories2008/20080124_iyor.html. .

Nugues, M. M., & R. P. M. Bak, 2006. Differential competitive abilities between Caribbean coral species and a brown alga: A year of experiments and a long-term perspective. Marine Ecology Progress Series 315: 75–86.

O'Neil, J. M., T. W. Davis, M. a. Burford, & C. J. Gobler, 2012. The rise of harmful cyanobacteria blooms: The potential roles of eutrophication and climate change. Harmful Algae Elsevier B.V. 14: 313–334, http://dx.doi.org/10.1016/j.hal.2011.10.027.

Paerl, H. W., P. T. Bland, N. D. Bowles, & M. E. Haibach, 1985. Adaptation to High-Intensity, Low-Wavelength Light among Surface Blooms of the Cyanobacterium Microcystis aeruginosa. Applied and environmental microbiology 49: 1046–1052.

Paerl, H. W., N. S. Hall, & E. S. Calandrino, 2011. Controlling harmful cyanobacterial blooms in a world experiencing anthropogenic and climatic-induced change. Science of the Total Environment Elsevier B.V. 409: 1739–1745, http://dx.doi.org/10.1016/j.scitotenv.2011.02.001.

Paerl, H. W., & V. J. Paul, 2012. Climate change: Links to global expansion of harmful cyanobacteria. Water Research Elsevier Ltd 46: 1349–1363, http://dx.doi.org/10.1016/j.watres.2011.08.002.

Pandolfi, J. M., 2003. Global Trajectories of the Long-Term Decline of Coral Reef Ecosystems. Science 301: 955–958, http://www.sciencemag.org/cgi/doi/10.1126/science.1085706.

Raps, S., K. Wyman, H. W. Siegelman, & P. G. Falkowski, 1983. Adaptation of the Cyanobacterium Microcystis aeruginosa to Light Intensity. Plant physiology 72: 829–832.

Rejmánková, E., & J. Komárková, 2000. A function of cyanobacterial mats in phosphorus-limited tropical wetlands. Hydrobiologia 431: 135–153.

Riding, R., 2000. Microbial carbonates: The geological record of calcified bacterial-algal mats and biofilms. Sedimentology 47: 179–214.

Roberts, C. M., C. J. McClean, J. E. N. Veron, J. P. Hawkins, G. R. Allen, D. E. McAllister, C. G. Mittermeier, F. W. Schueler, M. Spalding, F. Wells, C. Vynne, & T. B. Werner, 2002. Marine biodiversity hotspots and conservation priorities for tropical reefs. Science (New York, N.Y.) 295: 1280–1284.

Sampath-Wiley, P., & C. D. Neefus, 2007. An improved method for estimating R-phycoerythrin and R-phycocyanin contents from crude aqueous extracts of Porphyra (Bangiales, Rhodophyta). Journal of Applied Phycology 19: 123–129.

Schlüter, L., T. L. Lauridsen, G. Krogh, & T. Jørgensen, 2006. Identification and quantification of phytoplankton groups in lakes using new pigment ratios - A comparison between pigment analysis by HPLC and microscopy. Freshwater Biology 51: 1474–1485.

Schopf, J. W., 2000. The fossil record: tracing the roots of the cyanobacterial lineage The Ecology of Cyanobacteria. Kluwer Academic Publishers, Dordrecht, The Netherlands: 13–35.

Six, C., J.-C. Thomas, L. Garczarek, M. Ostrowski, A. Dufresne, N. Blot, D. J. Scanlan, & F. Partensky, 2007. Diversity and evolution of phycobilisomes in marine Synechococcus spp.: a comparative genomics study. Genome biology 8: R259.

Slattery, M., M. P. Lesser, D. Brazeau, M. D. Stokes, & J. J. Leichter, 2011. Connectivity and stability of mesophotic coral reefs. Journal of Experimental Marine Biology and Ecology Elsevier B.V. 408: 32–41, http://dx.doi.org/10.1016/j.jembe.2011.07.024.

Slijkerman, D. M. E., R. De León, & P. De Vries, 2014. A baseline water quality assessment of the coastal reefs of Bonaire, Southern Caribbean. Marine Pollution Bulletin Elsevier Ltd 86: 523–529, http://dx.doi.org/10.1016/j.marpolbul.2014.06.054.

Smith, S. E., D. W. Au, & C. Show, 1998. Marine Freshwater Research &. Fisheries (Bethesda) .

Stal, L. J., 1995. Physiological Ecology of Cyanobacteria in Microbial Mats and Other Communities. New Phytologist 131: 1–32.

Su, X., & P. G. Fraenkel, 1992. Excitation Energy Transfer from Phycocyanin to Chlorophyll in an upcA-defective Mutant of. 22944–22950.

Tandeau de Marsac, N., 1977. Occurence and nature of chromatic adaption in cyanobacteria. Journal of bacteriology 130: 82–91.

Ueno, Y., S. Aikawa, A. Kondo, & S. Akimoto, 2015. Light adaptation of the unicellular red alga, Cyanidioschyzon merolae, probed by time-resolved fluorescence spectroscopy. Photosynthesis Research Springer Netherlands 125: 211–218, http://link.springer.com/10.1007/s11120-015-0078-0.

Whitton, B. A., & M. Potts, 2000. The Ecology of Cyanobacteria: their Diversity in Time and Space. Kluwer Academic Publishers, Dordrecht, The Netherlands.

Wright, S. W., 1991. Improved HPLC method for the analysis of chlorophylls and carotenoids from marine phytoplankton. Marine Ecology Progress Series 77: 183–196.

Appendix

Explanation water samples and division BCM samples (Extra part of Materials & Methods)

This is the sample procedure of samples taken during the fieldwork of samples that are not analysed for this report.

Water samples

At spot 'C' water samples were taken by a Niskin Bottle lowered on a winch from the boat (Figure 5). The water samples were taken around 65m depth and approximately 7 meters above the ocean floor, to prevent contamination of the water samples with organic material from the ocean floor. After the Niskin Bottle was lifted into the boat, a 100ml syringe was filled with the sampled water.
At spot A and B water samples were taken with a 100 ml syringe while diving (Figure 5). When a sufficient cyanobacterial mat was found, the syringes were first three times rinsed with ocean water, to dispose any organic matter. Water samples were then taken 10 centimetres above the mat (Figure 18 in appendix), to prevent contamination of the water samples with organic material, raised into suspension by touching the cyanobacterial mat. After this, a water sample 5 meters perpendicular to the reef was taken as an extra reference sample (Figure 18 in appendix). The syringes were put in a dark garbage bag to prevent the water from light damage.
After the syringes were filled, multiple vials were filled for different analyses, which are explained hereafter. Afterwards the syringes were three times rinsed with tap water.

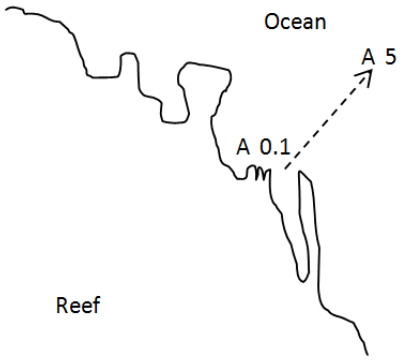

Figure 18. Position of the two different water samples. A 0.1 is a water samples taken 10 centimetres above the BCM. A 5 is the water samples taken 5 meters perpendicular to the reef

Nutrient samples

To perform nutrient analysis, two 5ml vials were filled with seawater. One vial will be used to measure dissolved tN/tP and one vial will be used to measure dissolved PO_4/NH_4/NO_3/NO_2. The vials were filled by attaching an Acrodisc to the syringe, to filter the water from any organic matter. Before filling the vials, first the Acrodisc, the vials and their lid were rinsed. After the vials were filled, they were stored upright in the dark at -20°C and transported to the Netherlands in a Bio-Freeze bottle.

DOC samples

After the nutrient sample was taken, a 30ml glass vial was, while using the Acrodisc, filled with 20ml filtered seawater and twelve drops of HCl were added. The DOC sample was stored in the dark at 4°C and transported to the Netherlands in a cool box.

TOC samples

After the DOC sample was taken, the Acrodisc was removed and a 30 ml glass vial was filled with 20ml filtered seawater. Again, twelve drops of HCl were added. The TOC sample was stored in the dark at 4°C and transported to the Netherlands in a cool box.

Cyanobacterial mat samples

It was found that the best way to collect the cyanobacterial mat samples was to put them with a fork in a tea sieve, shake a few times to lose a part of the sand through the sieve, and then put the cyanomaterial in a plastic Ziploc bag. This action was repeated until a sufficient amount of BCM was collected. This simple method was particularly useful at depth, since here the sampling time was limited to 3 minutes per replicate. All samples were taken in triplicate and at least 1 meter apart. Judged by their colour, mats with the highest biomass were chosen. The Ziploc bags were put in a dark garbage bag, to prevent the cyanobacterial samples from light damage. After the dive, the Ziploc bags were put in a cool box and multiple vials were filled for different analyses (Table 12), which are explained hereafter. Hereby gloves were worn and a pair of tweezers was used to allocate the cyanomaterial, thereby minimizing the amount of sand and seawater.

Pigment samples

Per sample a 2ml plastic vial was filled with cyanomaterial, to perform analysis on pigments and phycobilisomes. The samples were stored in the dark at -20°C and transported to the Netherlands in a Bio-Freeze bottle.

DNA samples

Per sample a 2ml plastic vial was filled with cyanomaterial, to identify the different organisms present in the cyanobacterial mat. The vials were filled up with molecular ethanol, to preserve the DNA in the sample. They were stored in the dark at 4°C and transported to the Netherlands in a cool box.

Visual check samples

An extra 2ml plastic vial was filled with cyanomaterial and a low amount of seawater, adding a drop of Lugol to make it possible to perform a visual check if this was needed. The samples were stored in the dark at 4°C and transported to the Netherlands in a cool box.

CNP samples

Material to perform CNP analysis on, was later on derived from the pigment samples.

Stable isotopes samples

A small Ziploc back (7x15 cm) was filled with the remaining cyanomaterial, to perform stable isotope analysis on. The samples were stored in the dark at -20°C and transported to the Netherlands in a Bio-Freeze bottle.

Table 12. Overview of the samples collected per samples spot. The column 'Samples' indicate the spot where the samples were taken. The number after the spot '(x)' indicates the number of sample locations of this type of spot. A total of 864 storage units were filled.
* The CNP samples were not taken separately, but derived from the pigment samples.

Samples	Nutrients	DOC	TOC	Pigments	DNA	Visual check	CNP sample*	Stabile isotopes
Deep (9)	12	6	6	3	3	3	3	3
Shallow (9)	12	6	6	3	3	3	3	3
Control (3)	6	3	3					
Total	234	117	117	54	54	54		54

Hydrolab PAR light curve on land

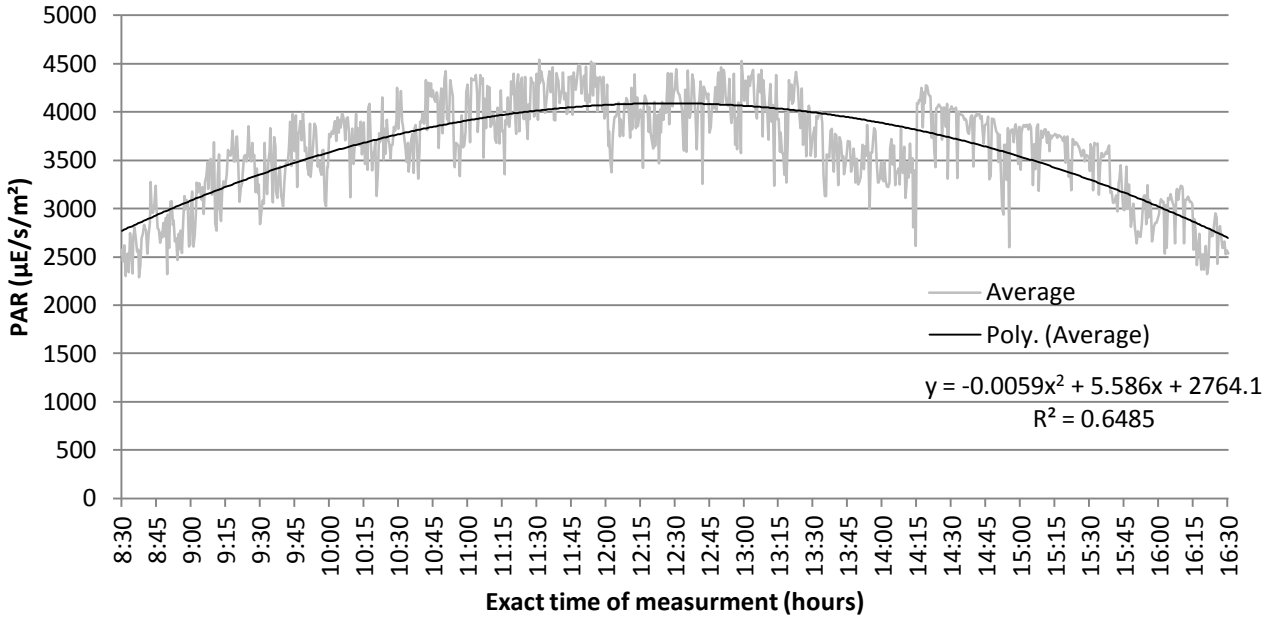

An average light curve created from four to seven land measurements (measured on 4, 10, 11, 13, 14, 16 and 17th of may 2015). A polynomial trend line has been fitted on the average data in excel. The average PAR light curve starts at 8:30 in the morning and ends at 16:30 in the midday

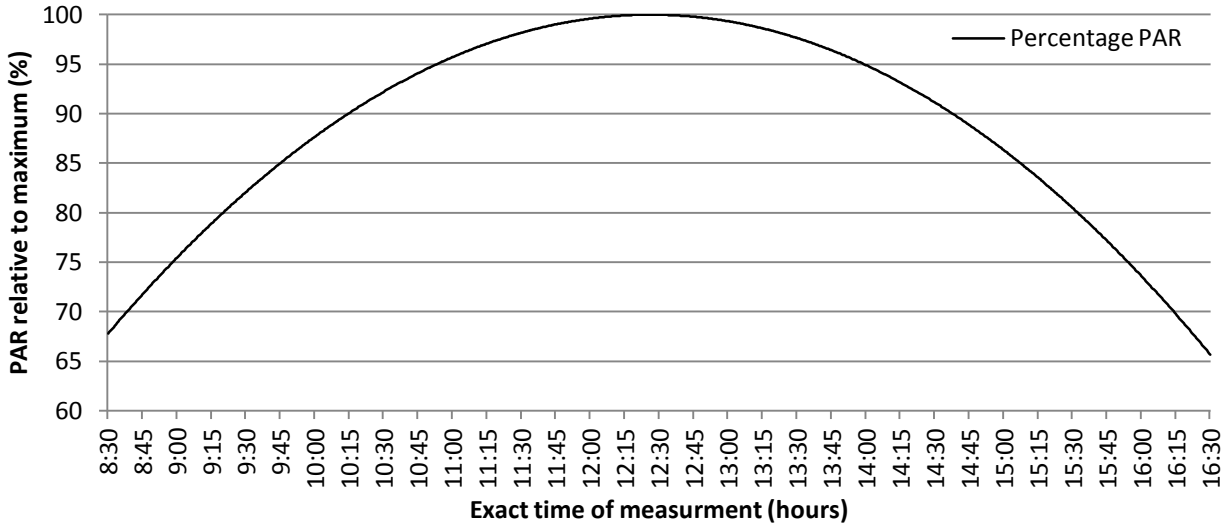

The polynomial trend line created by excel, based on the average data of seven land measurements, shown as a percentage of the maximum PAR. The trend line starts at 8:30 in the morning, ends at 16:30 in the midday and 100% PAR was reached at 12:26:00

RAMSES light intensity graphs

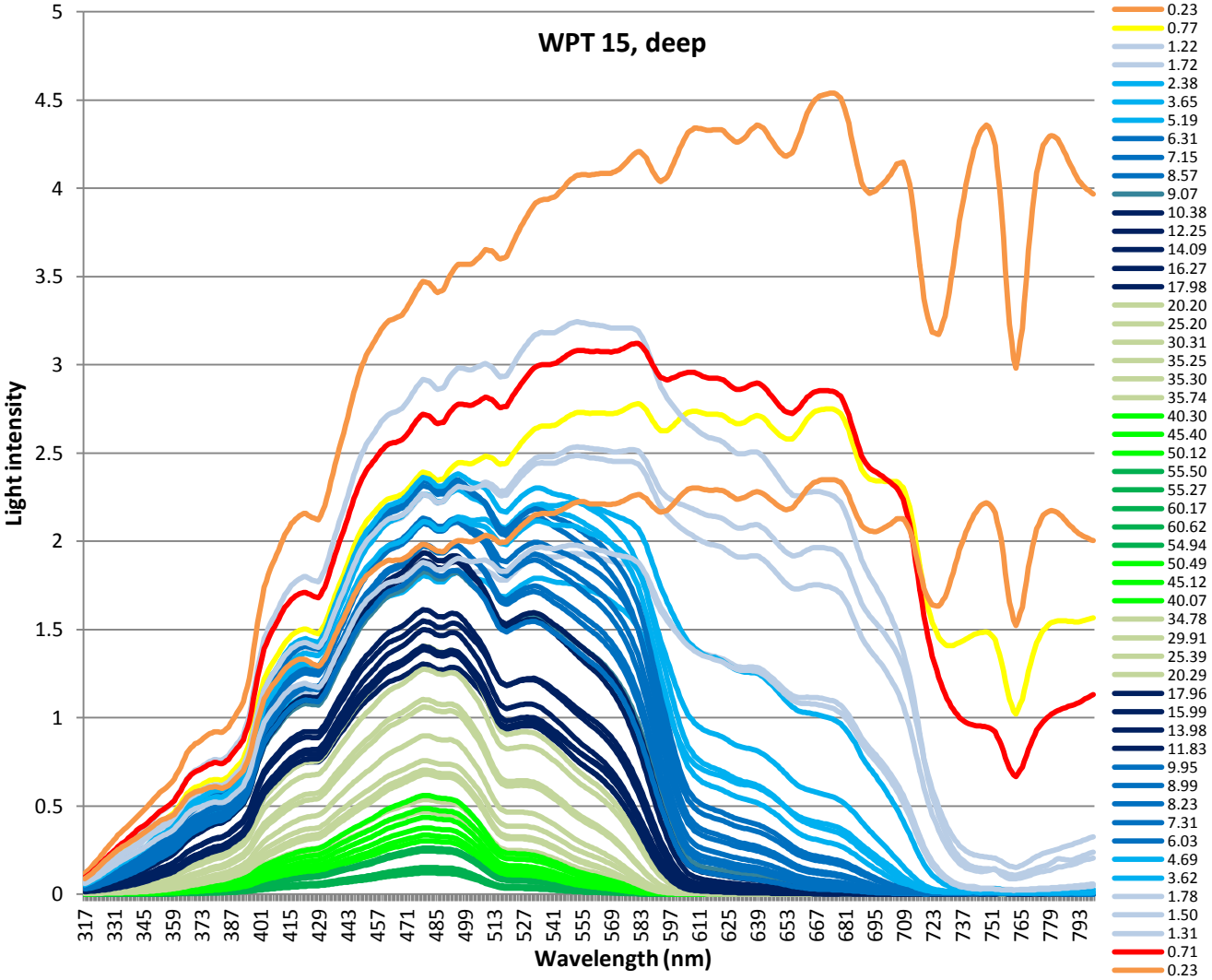

An example of a light intensity graph, containing all measurements of a deep deployment. The different colours indicate the different depth groups, according to Table 6. For every WPT, all measurements in one depth group were averaged, to create more readable and reliable graphs, shown hereafter. The legend contains the depth of each measurement

RAMSES light intensity graphs (data averaged per depth group)

The following graphs show the data averaged per depth group and relative to the surface light (corrected for by the first measurement under the water surface) per WPT. Dashed lines represent measurement taken during the shallow deployment, solid lines represents measurements taken during the deep deployment. The legend contains the average depth of each depth group. The last graph shows the group averages of the three control measurements, WPT 39 (———), WPT 44 (- - - - -) and WPT 56 (— · — · —).

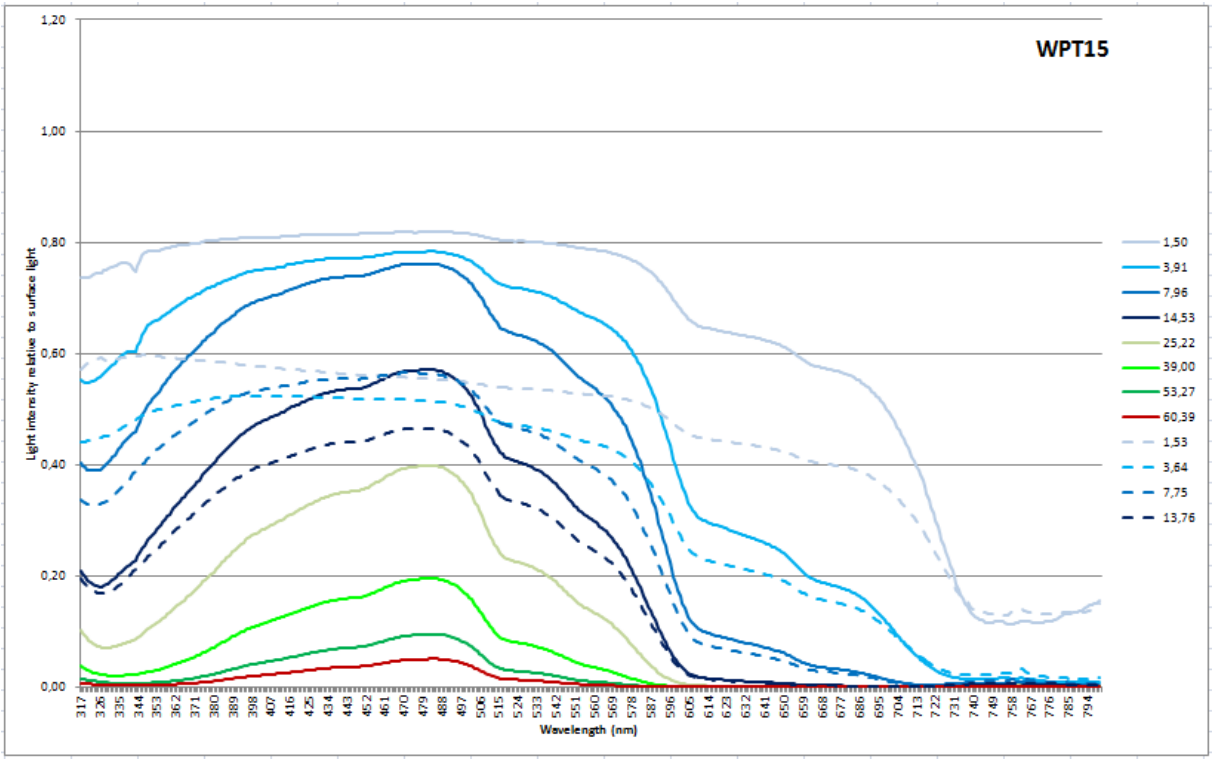

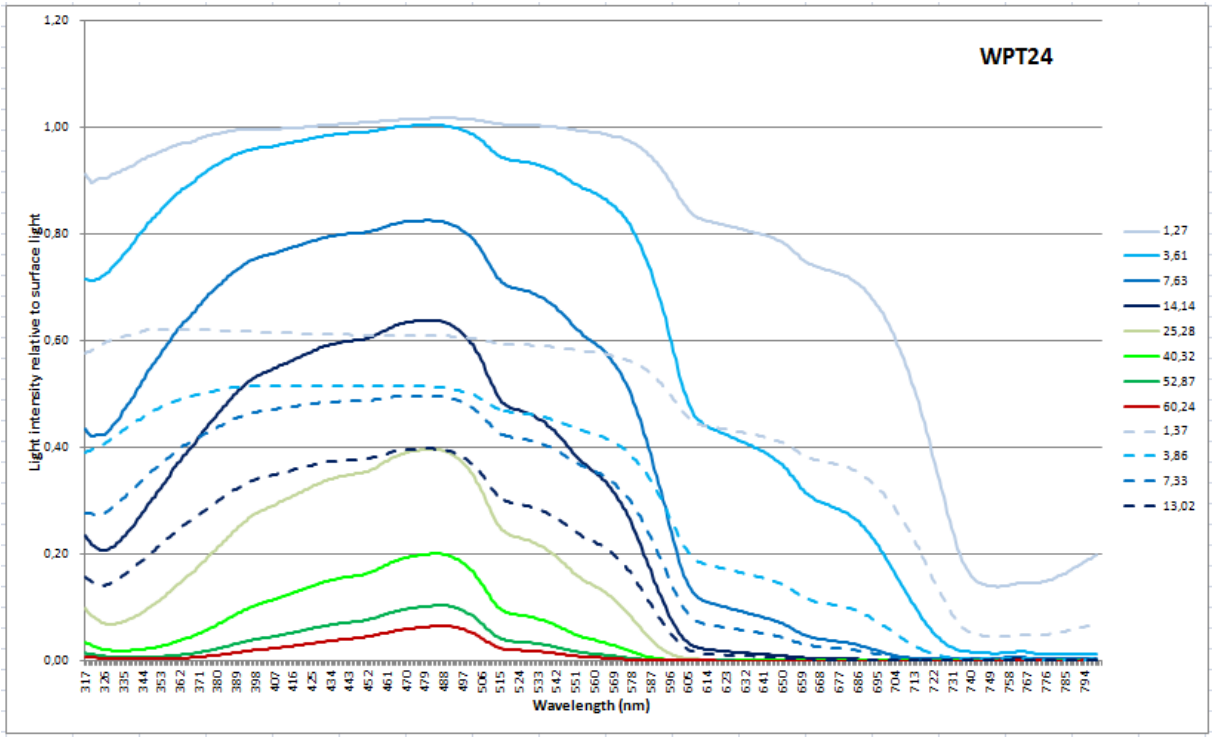

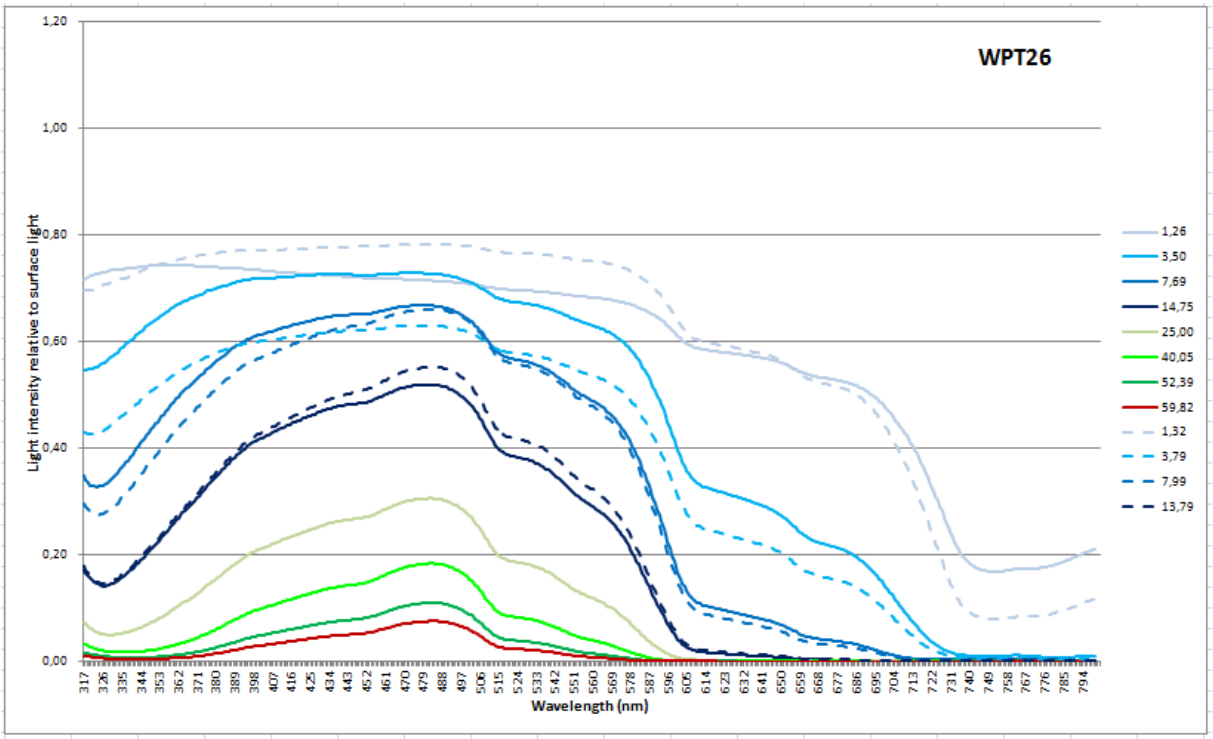
WPT26
Light intensity relative to surface light
Wavelength (nm)
1,26
3,50
7,69
14,75
25,00
40,05
52,39
59,82
1,32
3,79
7,99
13,79

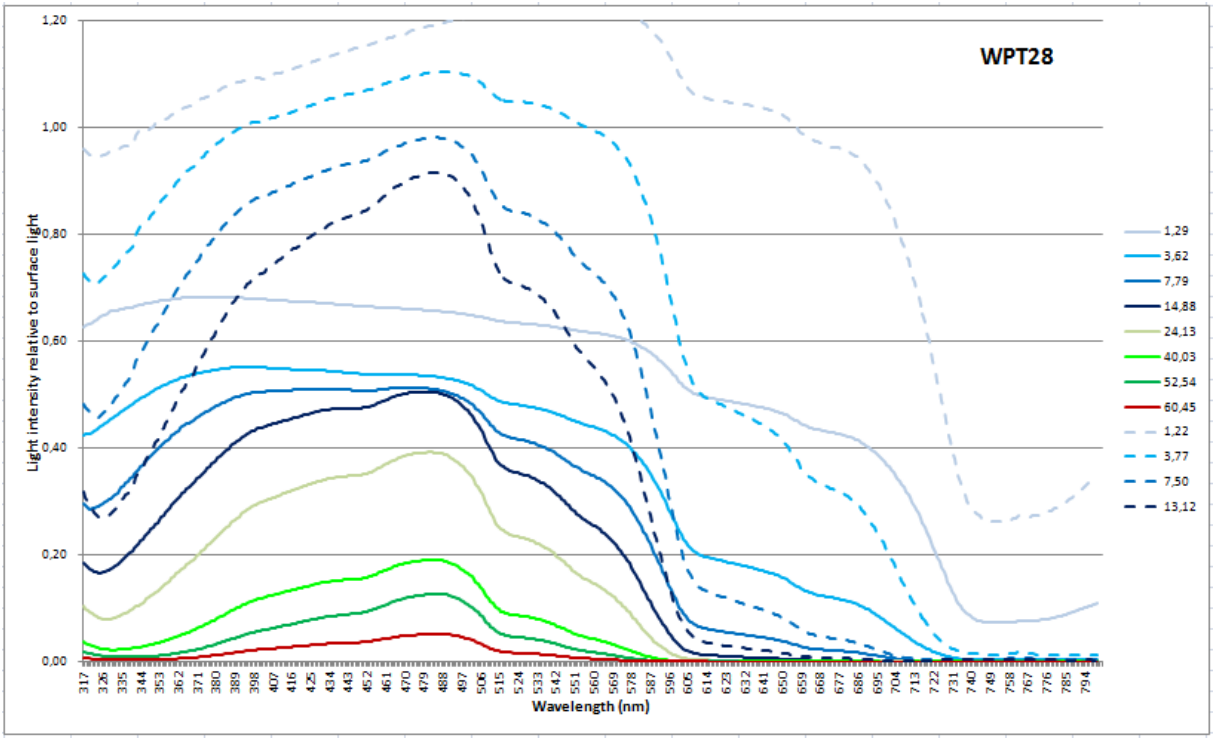
WPT28
Light intensity relative to surface light
Wavelength (nm)
1,29
3,62
7,79
14,88
24,13
40,03
52,54
60,45
1,22
3,77
7,50
13,12

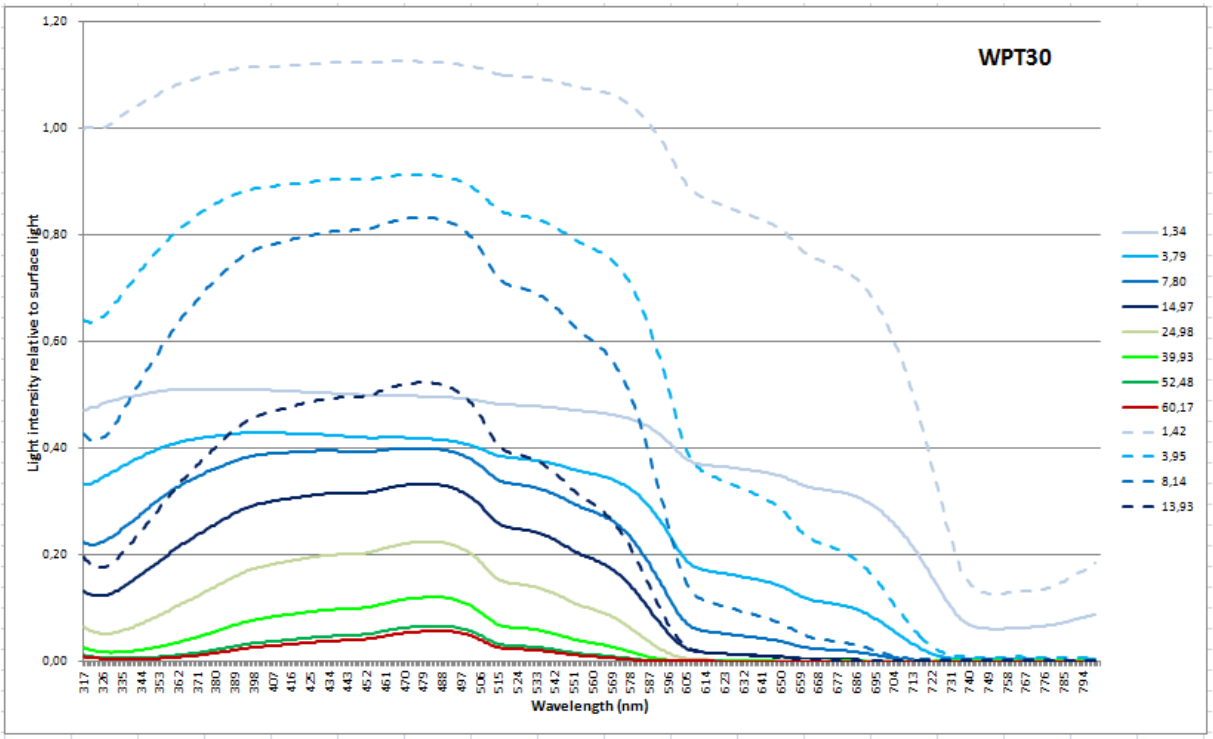
WPT30
Light intensity relative to surface light
Wavelength (nm)
1,34
3,79
7,80
14,97
24,98
39,93
52,48
60,17
1,42
3,95
8,14
13,93

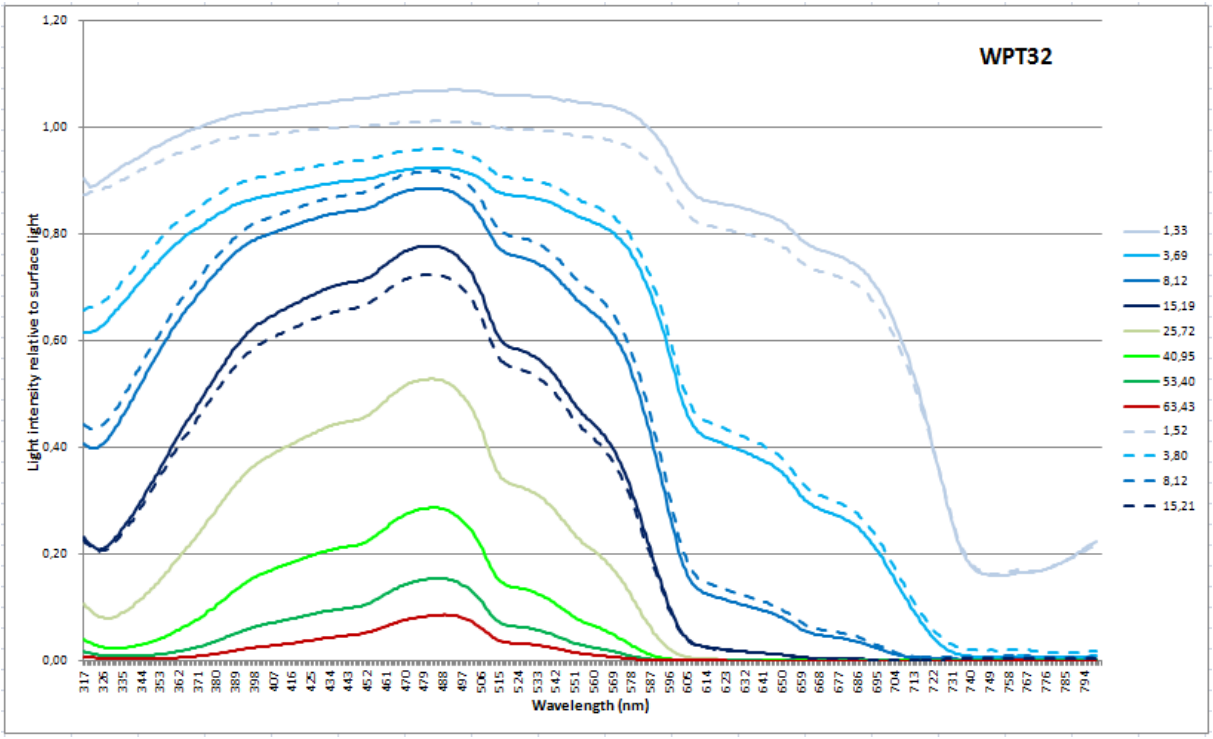
WPT32
Light intensity relative to surface light
Wavelength (nm)
1,33
3,69
8,12
15,19
25,72
40,95
53,40
63,43
1,52
3,80
8,12
15,21

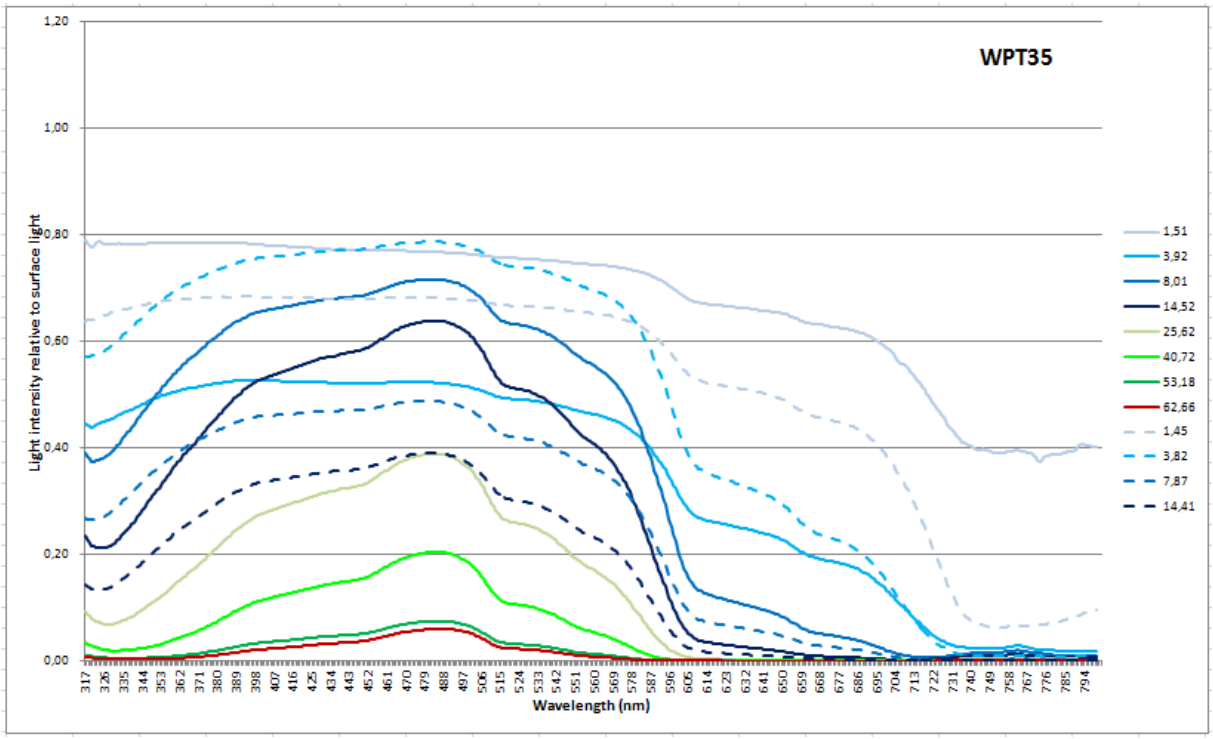
WPT35
Light intensity relative to surface light
Wavelength (nm)
1,51
3,92
8,01
14,52
25,62
40,72
53,18
62,66
1,45
3,82
7,87
14,41

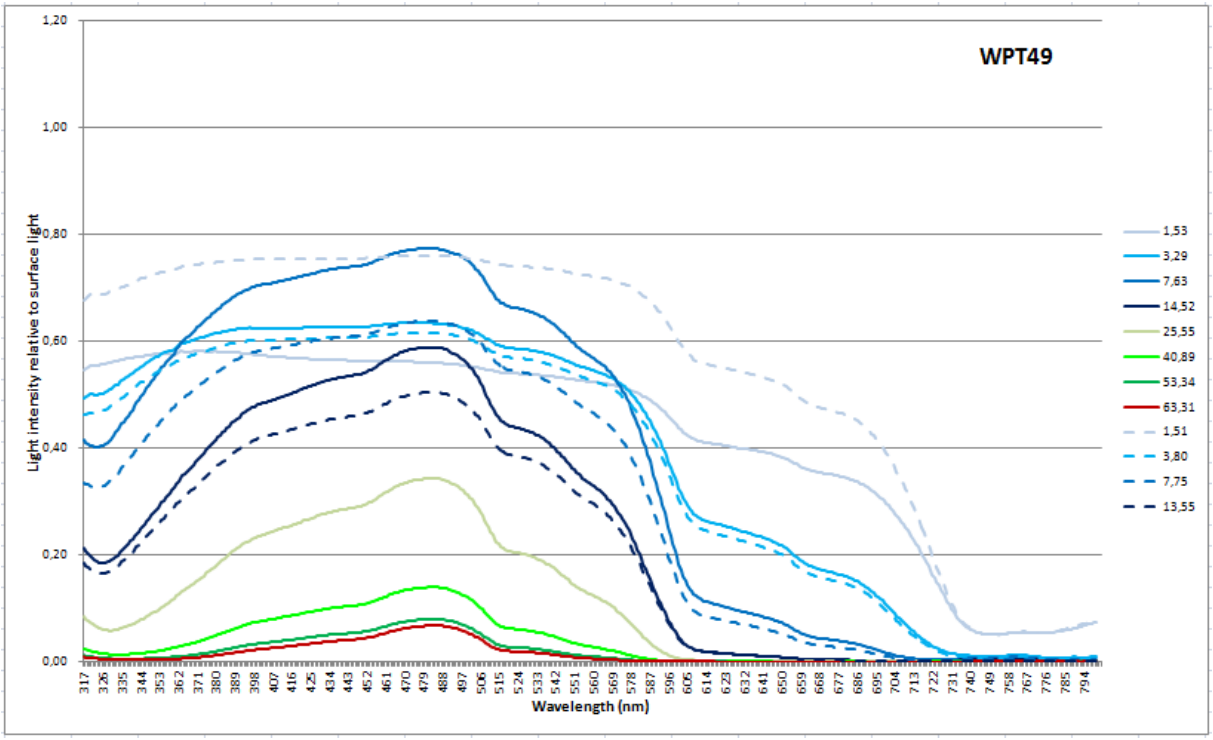
WPT49
Light intensity relative to surface light
Wavelength (nm)
1,53
3,29
7,63
14,52
25,55
40,89
53,34
63,31
1,51
3,80
7,75
13,55

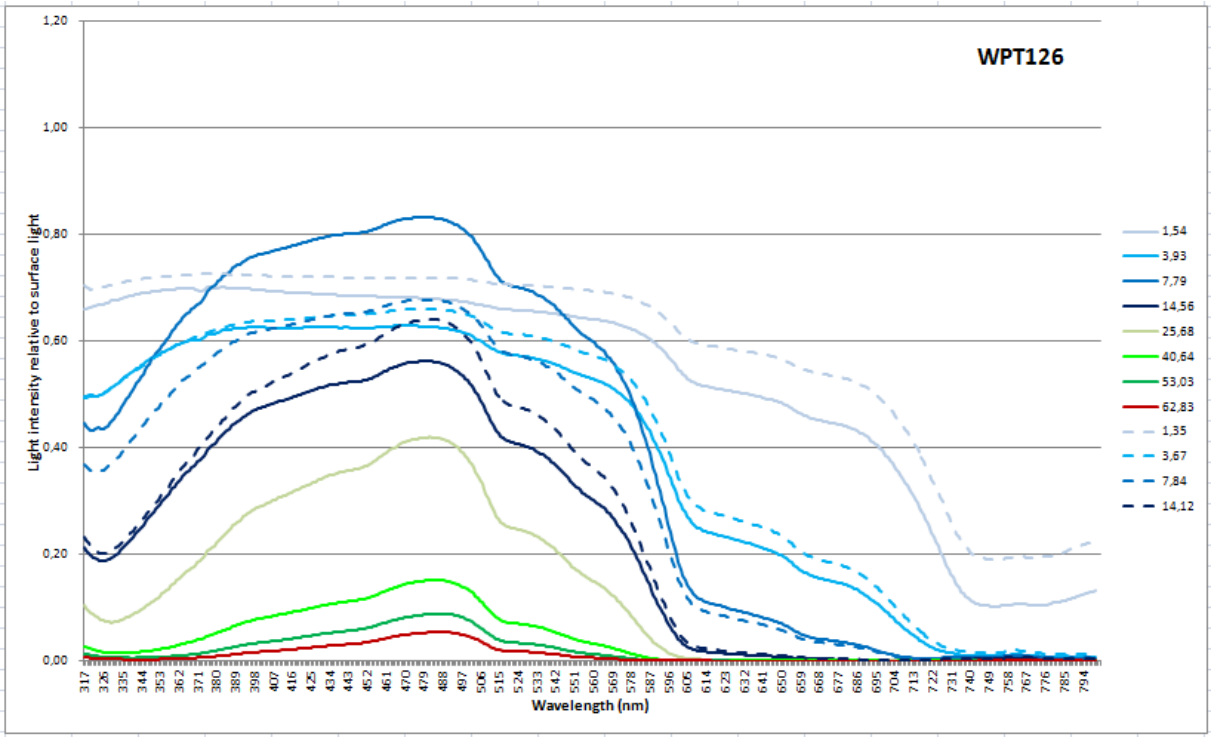
WPT126
Light intensity relative to surface light
Wavelength (nm)
1,54
3,93
7,79
14,56
25,68
40,64
53,03
62,83
1,35
3,67
7,84
14,12

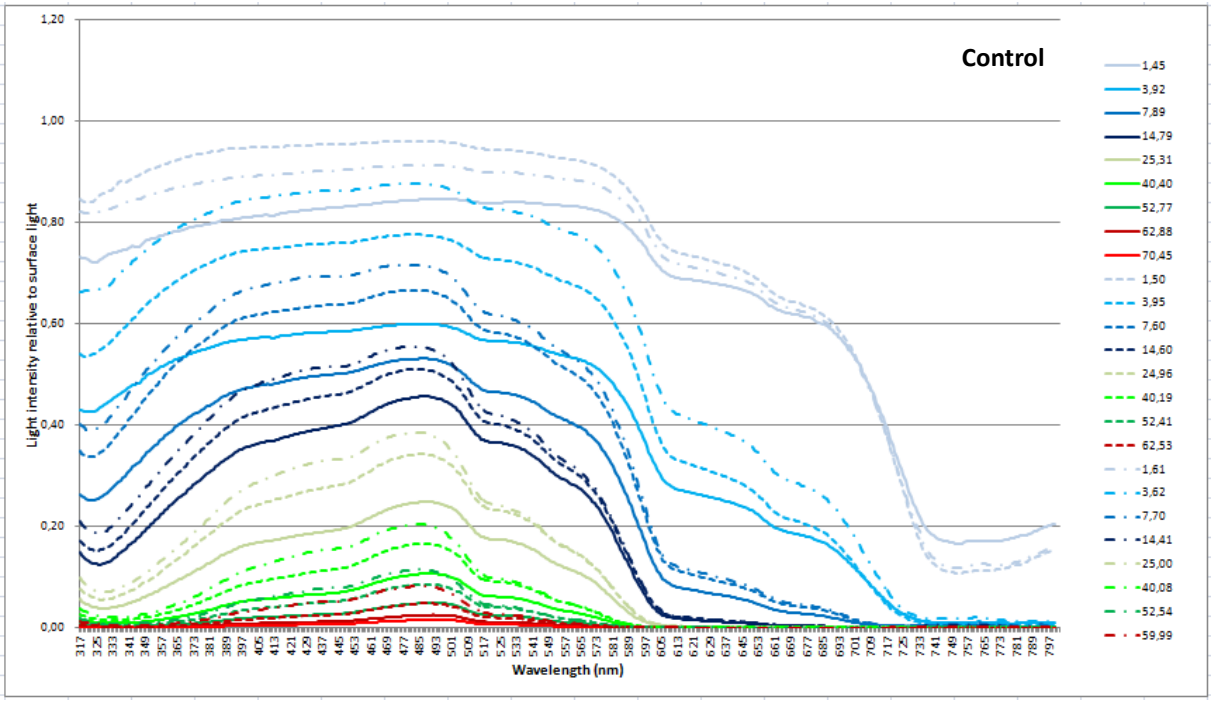
Control
Light intensity relative to surface light
Wavelength (nm)
1,45
3,92
7,89
14,79
25,31
40,40
52,77
62,88
70,45
1,50
3,95
7,60
14,60
24,96
40,19
52,41
62,53
1,61
3,62
7,70
14,41
25,00
40,08
52,54
59,99

Phycobilisome graphs

The following graphs show the amount of absorption, caused by phycobilisomes in 100µg AFDW, measured by an Aminco dual wavelength spectrophotometer. The measurements are run against buffer samples, the baseline was corrected and normalized to their lowest amount of absorption between 600 and 750 nm.

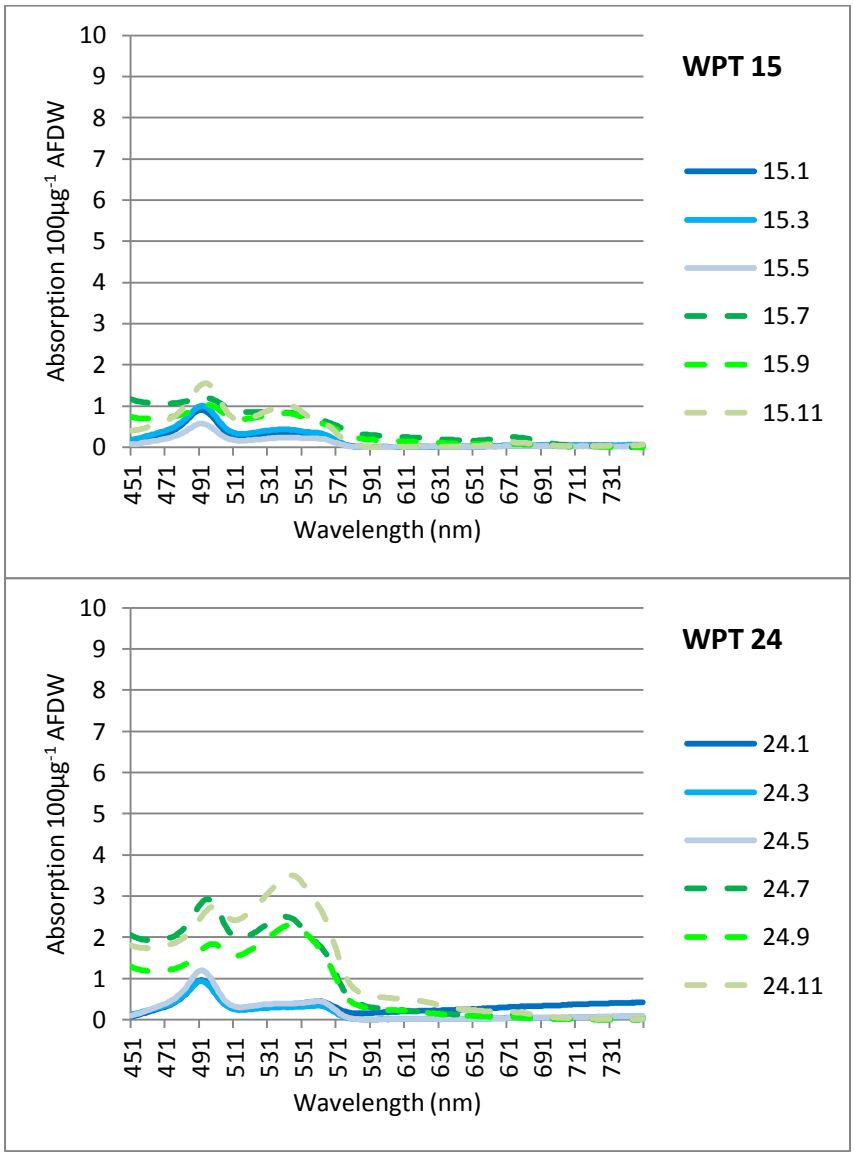

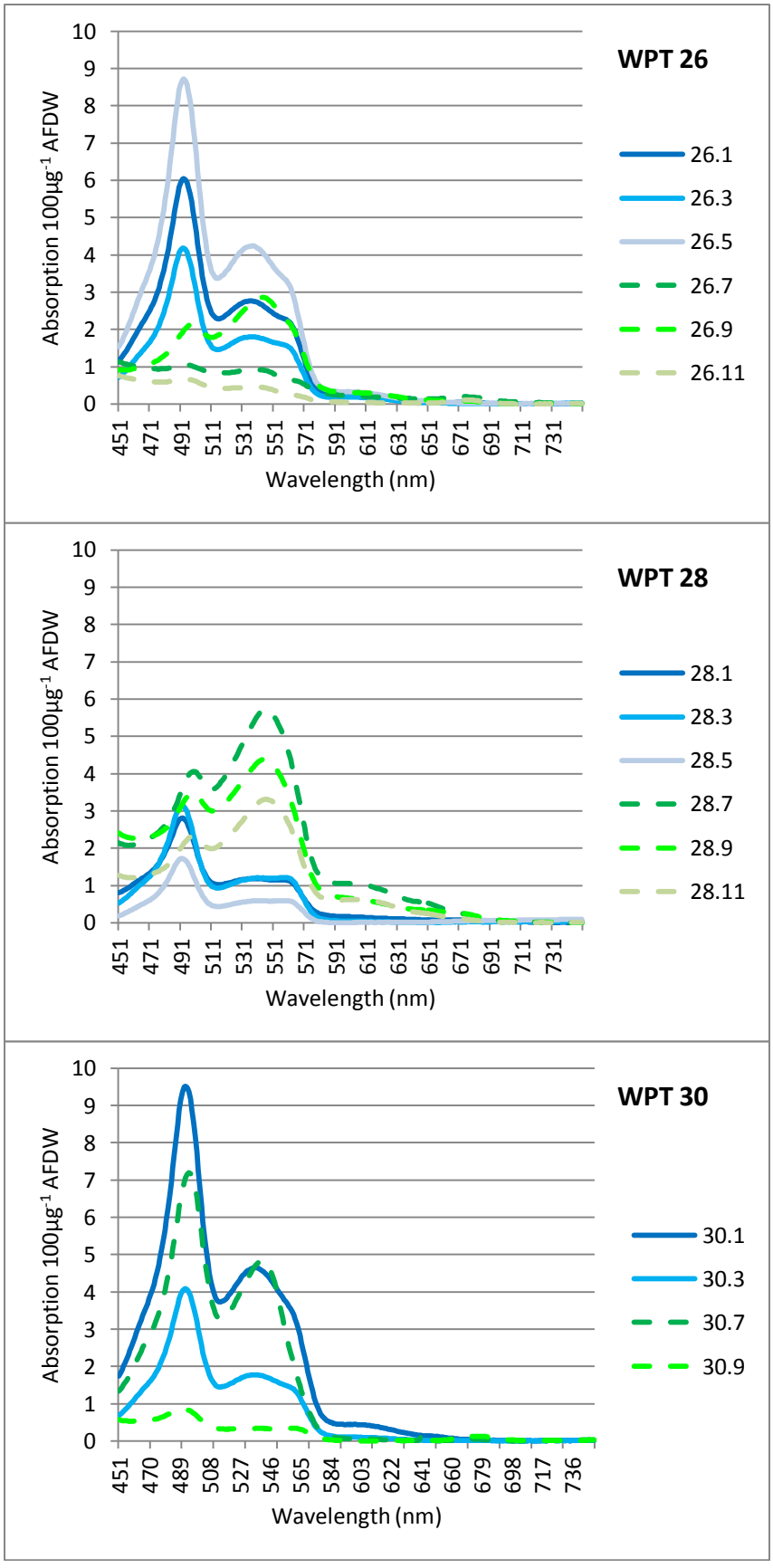
WPT 26
Absorption 100µg⁻¹ AFDW
Wavelength (nm)
26.1
26.3
26.5
26.7
26.9
26.11
WPT 28
Absorption 100µg⁻¹ AFDW
Wavelength (nm)
28.1
28.3
28.5
28.7
28.9
28.11
WPT 30
Absorption 100µg⁻¹ AFDW
Wavelength (nm)
30.1
30.3
30.7
30.9

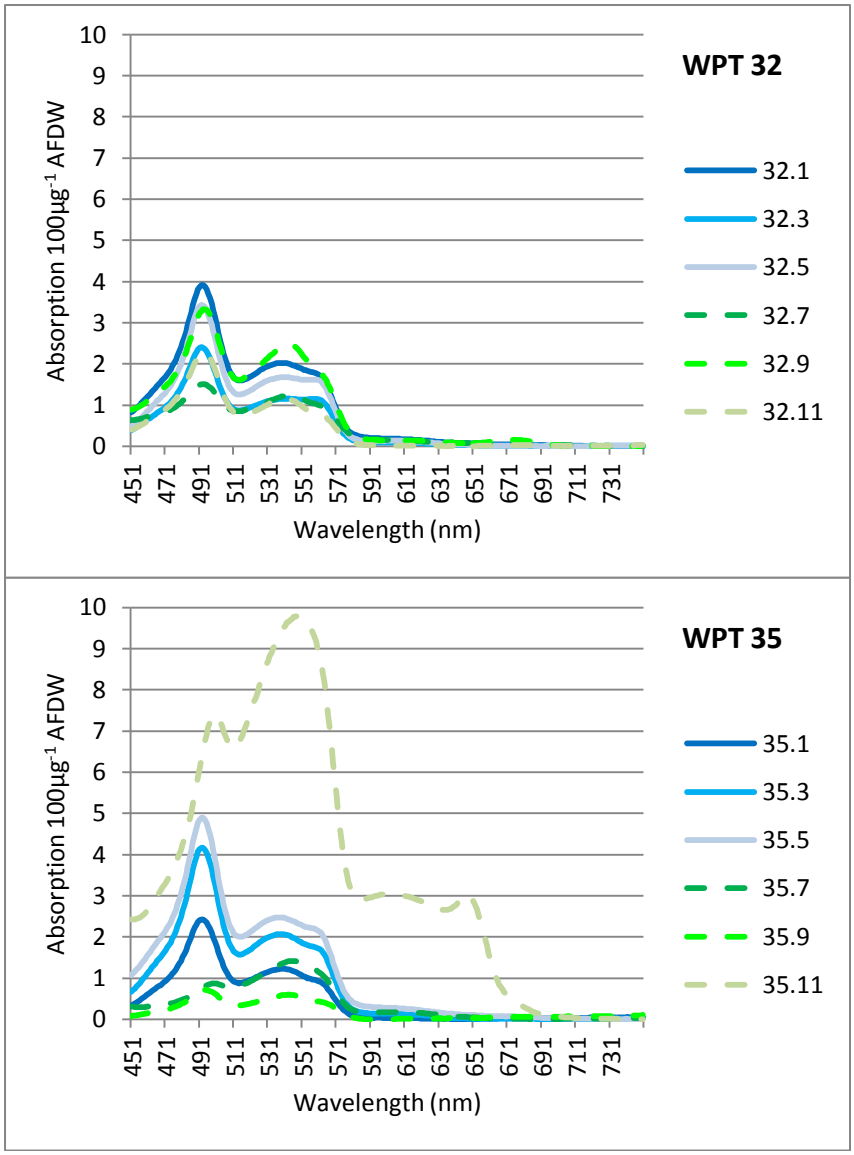
WPT 32
Absorption 100µg-1 AFDW
Wavelength (nm)
32.1
32.3
32.5
32.7
32.9
32.11
WPT 35
Absorption 100µg-1 AFDW
Wavelength (nm)
35.1
35.3
35.5
35.7
35.9
35.11

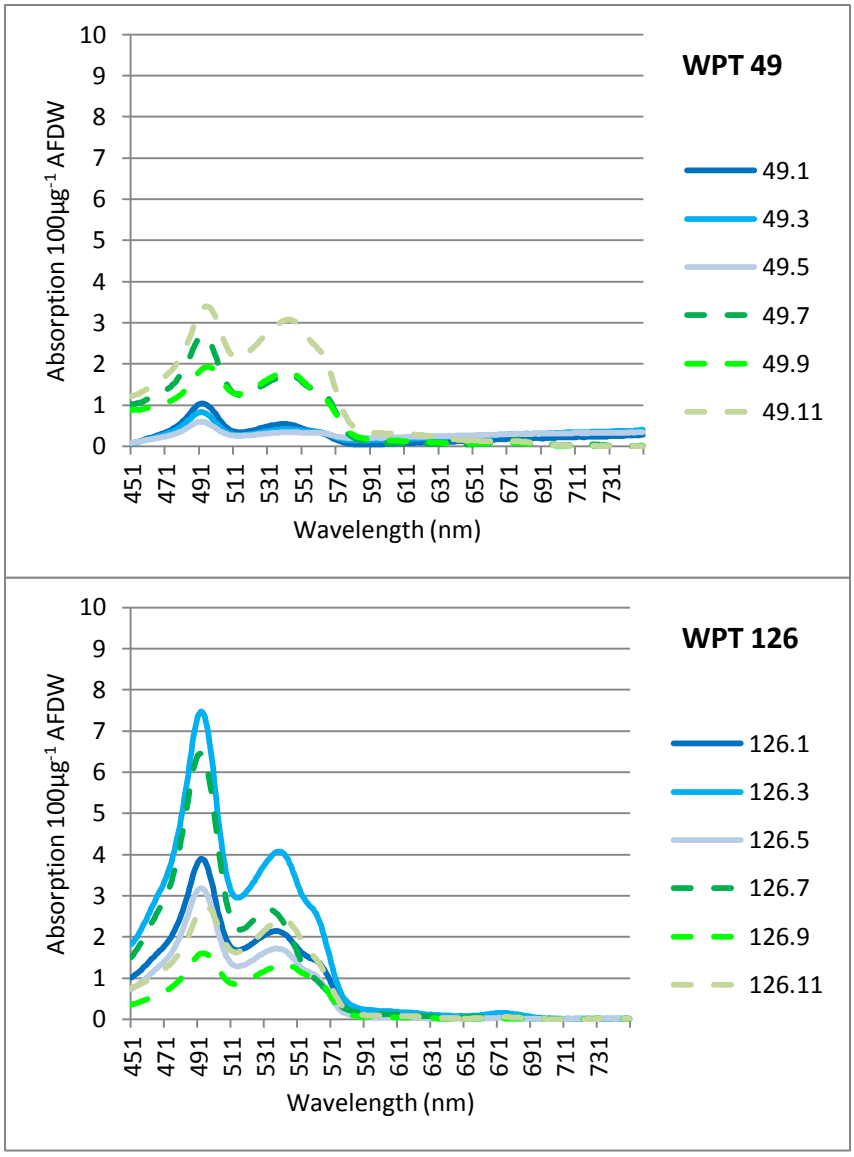
WPT 49
Absorption 100µg-1 AFDW
Wavelength (nm)
49.1
49.3
49.5
49.7
49.9
49.11
WPT 126
Absorption 100µg-1 AFDW
Wavelength (nm)
126.1
126.3
126.5
126.7
126.9
126.11

Hydrophobic pigments

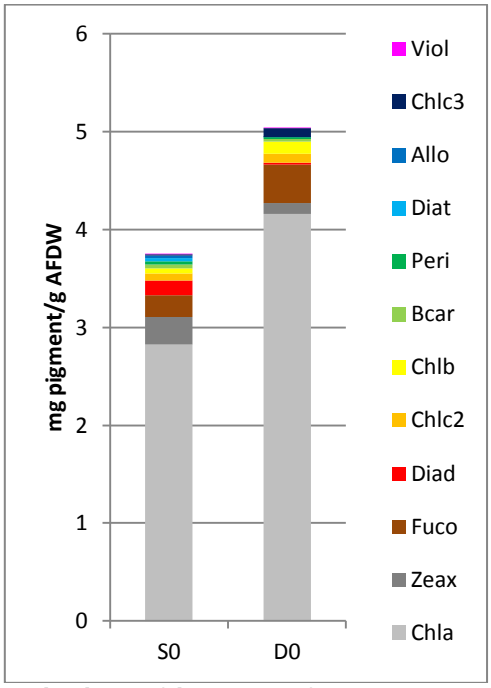

Stack column of the amount of pigments

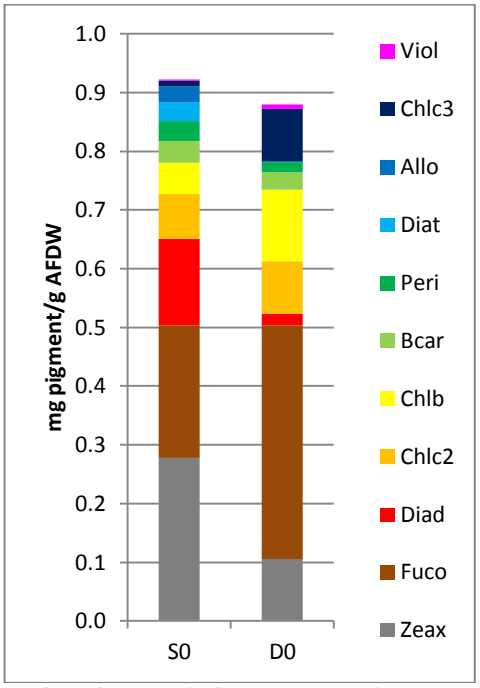

Stack column of the amount of pigments without Chlorophyll a